Technical Report 1671
September 1994

Structural Evaluation of TACAN/JTIDS/CDF Antenna Mast Assembly

R. C. Shaw

Technical Report 1671
September 1994

Structural Evaluation of TACAN/JTIDS/CDF Antenna Mast Assembly

R. C. Shaw

NAVAL COMMAND, CONTROL AND OCEAN SURVEILLANCE CENTER
RDT&E DIVISION
San Diego, California 92152–5001

K. E. EVANS, CAPT, USN
Commanding Officer

R. T. SHEARER
Executive Director

ADMINISTRATIVE INFORMATION

The work reported here was sponsored by the Space and Naval Warfare Systems Command, Program Executive Office, PMW-159, Arlington, VA 22245–5200. The work was funded under program element 0205604N and was performed during FY 1994.

Released by
A. R. Dean, Head
Mechanical Design Branch

Under authority of
R. E. Miller, Head
Sustainability Engineering Division

ACKNOWLEDGMENTS

The author wishes to express his sincere gratitude to J. E. Boyns of Code 753 for funding support and for his valuable suggestions and recommendations in organizing and editing the final report.

The author also would like to thank M. A. Jones of Code 813 for compiling the mass and stiffness properties of the pole mast and the CDF antenna mast assembly.

JA

SUMMARY

OBJECTIVES

To develop an effective computational method to analyze the dynamic behavior of the shipboard antenna mast assembly when subjected to the shock environment caused by a near-miss underwater explosion. The method should determine whether the vertical mast of the AS-3506A/SRS-1 Combat Direction Finder (CDF) antenna assembly (ADCOCK Configuration) can support both the AS-3240/URN Tactical Air Navigation (TACAN) antenna and the Joint Tactical Information Distribution System (JTIDS) antenna under the worst environmental condition aboard a ship.

RESULTS

A FORTRAN computer program called "MASTY" was developed to analyze the shock and vibration responses of the shipboard antenna mast assembly, which can be treated as a vertical cantilever beam having continuously distributed mass and nonuniformly distributed elasticity, in addition to carrying point masses. A two-part analysis procedure is implemented in MASTY: (1) a derivation of the system's equations of motion based on the well-known Rayleigh's method for the vibration analysis of structures, and (2) a numerical integration scheme for the solution to the equations of motion using Kutta-Merson's fourth-order predictor-corrector technique. The output format of MASTY is tailored so that the time-histories of the response variables and their shock spectra can be plotted with the personal computer code YADAP.

Two CDF antenna mast arrangements, the one with TACAN antenna alone on top of the mast and the other with both TACAN and JTIDS antennas, were analyzed with MASTY. The maximum responses of the two arrangements subjected to an 8-g/4-Hz idealized sinusoidal athwartship shock at the base of the pole mast (010 level), on top of which the CDF antenna mast assembly is mounted, are summarized in table I. The response variables included in table I are lateral displacement, acceleration, and angular rotation at the center of gravity of the TACAN antenna and shear force, bending moment, and the maximum flexural stress reacted at the base of the extender tube, which is considered to be the weakest link in the whole mast.

Table I. Summary of dynamic responses for two CDF antenna mast arrangements.

Antenna Arrangement	Natural Frequency	Athwartship Shock Input	Max TACAN Response	At Base of Ext Tube			Safety Margin
				Shear	Moment	Stress	
			Disp/Accel/Rotation	(lb)	(in-lb)	(psi)	
TACAN Alone	4.96 Hz	8 g/4 Hz	25.4"/51.5 g/11.4°	7,393	361,700	69,709	-0.05
TACAN/JTIDS	3.25 Hz	8 g/4 Hz	46.0"/61.1 g/19.6°	14,819	967,610	186,473	-0.65

CONCLUSION

Table I indicates that, under the shipboard shock environment considered, the modified Version-1 CDF antenna mast assembly with a Version-2 extender tube (4.615-inch outside diameter (OD) and 0.403-inch thick) is barely able to support the TACAN antenna alone. It cannot support both TACAN and JTIDS antennas in combination because of the excessive bending stress developed at the base of the extender tube by the shipboard shock.

RECOMMENDATIONS

A parametric study is performed in an attempt to raise the fundamental frequency of the system (with TACAN and JTIDS) by varying the thickness and/or the OD of the extender tube. The results of the study are summarized in table II. Table II shows that replacing the extender tube with a solid rod of the same OD can raise the natural frequency of the system by only 2.06%, while doubling both the OD and the thickness of the extender tube by only 5.45%. Obviously, changing the design of the extender tube alone is not an effective means of raising the natural frequency of the system. Better weight and stiffness distributions of the whole mast are required. The most effective way would be to perform a design optimization for the entire antenna mast assembly to arrive at a minimum weight design that meets a lower bound constraint on the fundamental frequency. This goal can be achieved via the "optimality criteria approach." In the optimality criteria approach, a criterion related to the behavior of the structure, such as the fundamental frequency in this case, is derived, and the premise is that when the structure is sized to satisfy this criterion, the merit function (structural weight) automatically attains an optimal value. This approach is strongly recommended here.

Table II. Sensitivity of the system's fundamental frequency to a design change in the extender tube.

Design Variation	OD/Thk (in/in)	Wt (lb)	EI/L^3 (lb/in)	System's Freq (Hz)	Percent Increase
Current Design	4.615/0.403	16.04	6.486	3.247	
Solid Rod	4.615/2.307	50.30	12.102	3.314	+2.06
Double OD & Thk	9.230/0.806	64.14	103.776	3.424	+5.45

The computer program MASTY developed for this study has provided an effective tool to analyze the dynamic behavior of the antenna mast assembly when subjected to shipboard shock. The current version of MASTY, however, can analyze the dynamic behavior of the mast in the athwartship direction (y-direction) only. It can be expanded to analyze the responses in the other two directions, i.e., the forward (x-direction) and the vertical (z-direction) motions.

CONTENTS

FIGURES

TABLES

SCOPE OF THE WORK

The purpose of this work is to analytically determine whether the vertical mast of the AS-3506A/SRS-1 Combat Direction Finder (CDF) antenna assembly (ADCOCK Configuration) can support both the AS-3240/URN Tactical Air Navigation (TACAN) antenna and the Joint Tactical Information Distribution System (JTIDS) antenna under the worst environmental condition aboard a ship. A FORTRAN computer program called MASTY has been developed by Code 813 to analyze the transient response of the antenna mast assembly subjected to the base motion caused by a near-miss underwater explosion, which is considered to be the cause of the worst-case shipboard shock. A two-part analysis procedure is implemented in MASTY: (1) a derivation of the system's equations of motion based on the well-known Rayleigh's method (reference 1) for the vibration analysis of structures, and (2) a numerical integration scheme for the solution to the equations of motion using Kutta-Merson's fourth-order predictor-corrector technique (reference 2). MASTY is dedicated to providing an efficient and accurate means of analyzing the shock and vibration responses of the shipboard antenna mast assembly, which can be treated as a vertical cantilever beam having continuously distributed mass and nonuniformly distributed elasticity, in addition to carrying point masses.

INTRODUCTION

As shown in figure 1, the CDF antenna assembly is mounted on top of a 14-degree tilted pole mast, which has a squared tubular section and a uniform wall thickness and carries three UHF antennas. The vertical mast of the CDF antenna assembly is composed of several tubular segments with different cross sections. The lower portion of the vertical mast is a short circular section with a constant outside diameter (OD) and a uniform wall thickness, except for the base flange, which has a larger OD for mounting to the pole mast. The remaining portion of the vertical mast is made of a long slender tubing that tapers slightly from the lower portion where the CDF antenna is mounted toward the upper one-third of the mast and has nonuniform wall thickness. The upper one-third of the vertical mast, which supports an array of dipole antennas, is of uniform cross section and has a wider flange at the top. The vertical mast is joined by an even more slender tubing on which a TACAN antenna assembly or JTIDS and TACAN antennas in series are mounted. However, uncertainty arises as to whether the current vertical mast design can support both JTIDS and TACAN antennas under the worst shipboard shock environment (a near-miss underwater explosion).

A commercial finite element analysis (FEA) program such as ABAQUS*, which is available on the Center-owned minisupercomputer STINGRAY, could have been used to analyze the ship-shock response for this type of structure. But, in order to maintain self-sufficiency and a high level of efficiency in repeated applications, a FORTRAN computer program was developed, which is dedicated to analyzing the dynamic behavior of this partially tapered cantilever beam having nonuniformly distributed elasticity and carrying point masses.

* ABAQUS is an FEA computer code that is a registered trademark of Hibbitt, Karlsson & Sorensen, Inc.

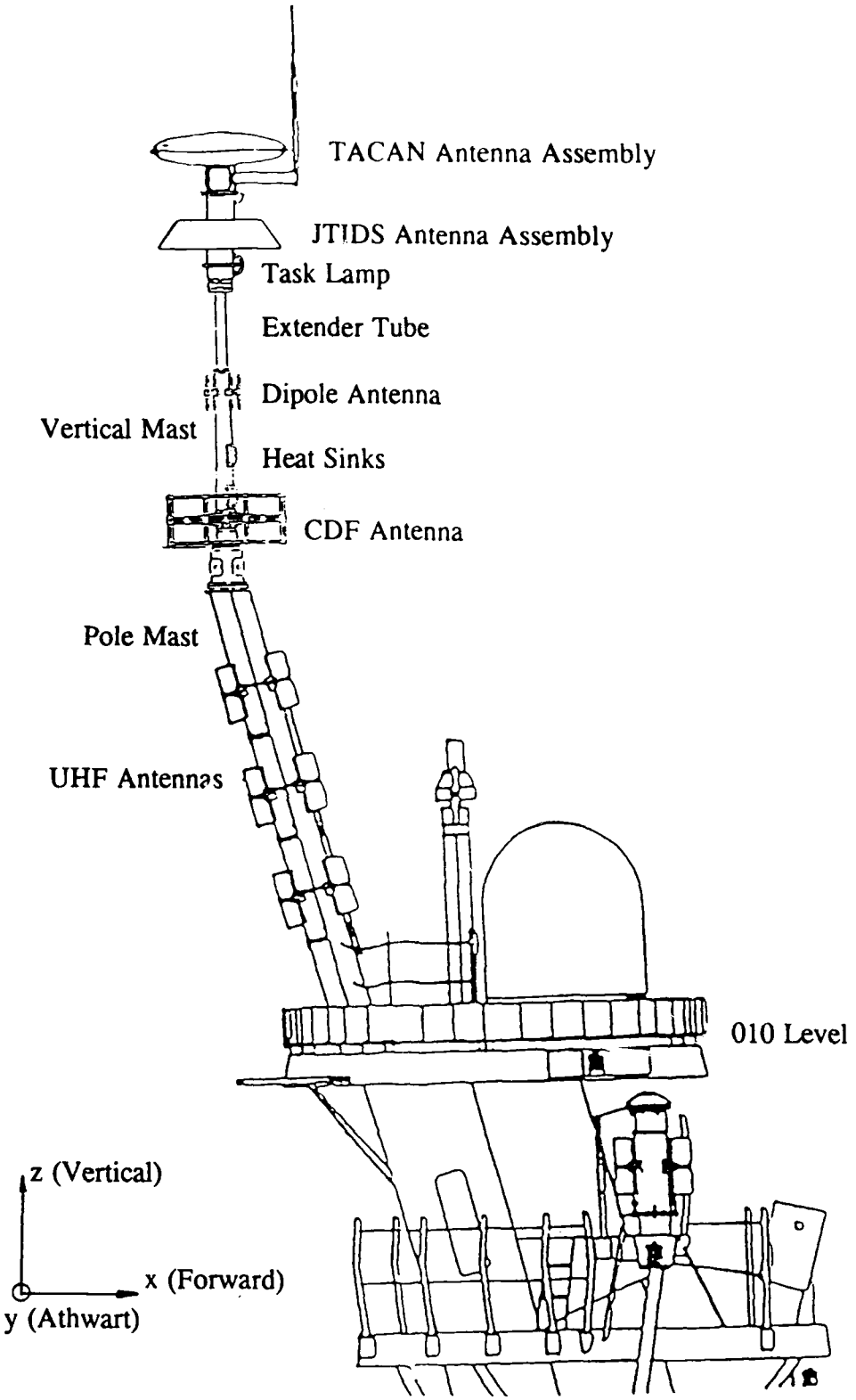

Figure 1. AS-3506A/SRS-1 CDF antenna assembly with TACAN and JTIDS antennas installed.

The analysis procedures implemented in this program are described in the next section. The analysis results, which include time-history plots of the response variables and their shock spectrum analyses using a Personal Computer (PC) code YADAP (reference 3), conclusions, discussions, and recommendations are presented in the subsequent sections.

ANALYSIS PROCEDURES

The analysis procedures implemented in MASTY consist of two parts: (1) a derivation of the system's equations of motion and fundamental frequency using Rayleigh's method, which models the antenna mast as a single-degree-of-freedom (SDOF) system through the use of an assumed displacement shape compatible with the support condition of the mast, and (2) a numerical integration scheme for the solution to the equations of motion using Kutta-Merson's fourth-order predictor-corrector technique. These procedures are described next.

RAYLEIGH'S METHOD

Theoretically, a continuous beam has an infinite number of degrees of freedom, and thus can displace in an infinite variety of displacement patterns during vibration. To apply Rayleigh's procedure, it is necessary to assume the shape that the beam will take in its fundamental mode of vibration. This assumption effectively reduces a continuous beam to an SDOF system that may deflect only in its fundamental mode. This assumption is acceptable for the shock and vibration analysis of the shipboard antenna mast, since the underwater explosion shock accentuates some frequency components and surpresses others when propagating through a structural path of the ship's hull, the deck, the superstructure, and the main mast before reaching the base of the pole mast (010 level). The motion data taken at the base of the pole mast during the CG-53 shock trials indicated that the athwart component (y-direction) of the motion was about 4 to 6 Hz and 8 to 12 g. This low-frequency motion is unlikely to excite any higher vibration mode of the CDF mast than its fundamental mode. Rayleigh's method is formulated as follows:

Consider an antenna mast, which has a flexural stiffness distribution EI(x) and a mass per unit length distribution m(x) and carries point masses M_i, is subjected to the base motion $v_g(t)$ as shown in figure 2. To approximate the motion of this system with an SDOF, it is necessary to assume that it may deflect only in a single shape. Thus, the motion at any point on the mast can be written as

$$v(x,t) = P(x)Z(t) \qquad (1)$$

in which P(x) is the shape function and Z(t) is the generalized coordinate representing the amplitude of the motion. Typically the generalized coordinate is selected as the displacement of some convenient reference point in the system, such as the displacement at the tip of the mast. The equations of motion of this generalized system can be derived by the principle of conservation of energy (Hamilton's principle), which states that the variation of the kinetic energy (T) and potential energy (V) plus the variation of the work done by the nonconservative

forces (W_{nc}) acting on the system, including damping and any arbitrary loads, during any time interval t_1 to t_2 must equal zero, i.e.,

$$\int_{t_1}^{t_2} \delta(T - V)dt + \int_{t_1}^{t_2} \delta W_{nc} dt = 0 \tag{2}$$

The kinetic energy of the vibrating mast shown in figure 2 is given by

$$T = 1/2 \int_0^L m(x)[\dot{v}_t(x,t)]^2 \, dx + 1/2 \sum M_i(\dot{v}_i)^2 \tag{3}$$

in which $\dot{v}_t = dv_t/dt$ represents the velocity vector of the total displacement relative to the reference axis, i.e., $v_t = v + v_g$, and $\dot{v}_i$ represents the velocity at point mass M_i. The potential energy for the flexural deformation of the mast is given by

$$V = 1/2 \int_0^L EI(x)[v''(x,t)]^2 \, dx \tag{4}$$

in which v" represents d^2v/dx^2. In the system of figure 2, there are no directly applied dynamic loads, and damping has been neglected; thus there are no nonconservative forces to be considered in Eq. (2). Now noting the relationships

$$\dot{v}_t = \dot{v} + \dot{v}_g \qquad v'' = p''Z \qquad v' = P'Z \qquad \dot{v} = P\dot{Z}$$

$$\delta\dot{v}_t = \delta\dot{v} \qquad \delta v'' = P''\delta Z \qquad \delta v' = P'\delta Z \qquad \delta\dot{v} = P\delta\dot{Z}$$

and substituting Eqs. (3) and (4) into (2), performing the indicated variations and integrating the first two terms by parts leads to

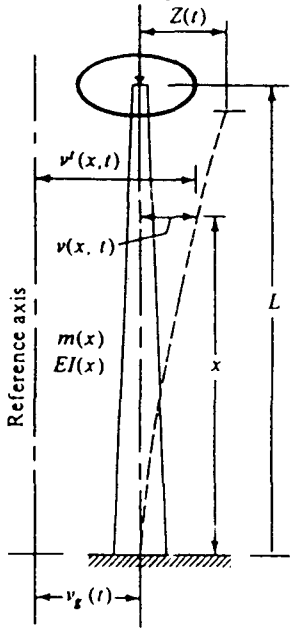

Figure 2. Antenna mast treated as an SDOF system.

$$\int_{t_1}^{t_2} [m^*\ddot{Z} + k^*Z - p^*(t)]\,\delta Z dt = 0 \tag{5}$$

in which $$m^* = \int_0^L m(x)P^2 dx + \sum M_i(P_i)^2 \tag{6a}$$

$$k^* = \int_0^L EI(x)(P'')^2 dx \tag{6b}$$

$$p^*(t) = -\ddot{v}_g(t)\left[\int_0^L m(x)P dx + \sum M_i(P_i)\right] \tag{6c}$$

are generalized mass, generalized stiffness, and generalized effective load, respectively. But since the variation Z is arbitrary, the term in brackets of Eq. (5) must vanish; hence the equation of motion of the generalized system finally may be written

$$m^*\ddot{Z}(t) + k^*Z(t) = p^*(t) \tag{7}$$

from which the natural frequency of the vibrating mast can be obtained

$$f_1 = (1/6.2832)\sqrt{k^*/m^*} \tag{8}$$

NUMERICAL SOLUTION TECHNIQUE

The second-order ordinary differential equation given by Eq. (7), which governs the dynamics of the amplitude Z(t) of the vibrating mast excited by the base acceleration $\ddot{v}_g(t)$ given by Eq. (6), can be solved numerically with the Differential Equation Solver (DEQS) implemented in MASTY. DEQS (reference 4) is an explicit numerical integration routine using Kutta-Merson's fouth-order predictor-corrector technique. The technique has been used successfully in analyzing the shipboard shock simulation tests for the nosecaps of Vertical Launch ASROC (reference 5). The solution process of DEQS begins with reducing each of the two second-order differential equations, Eqs. (6) and (7), into two first-order equations in terms of the state vectors Z(i), i = 1 to 4, which represent the displacements and velocities at the base and at the tip of the mast such that

$$\text{at the base} \quad dZ(1)/dt = Z(2) \quad \text{and} \quad dZ(2)/dt = \ddot{v}_g(t) \tag{9}$$

$$\text{and at the tip} \quad dZ(3)/dt = Z(4) \quad \text{and} \quad dZ(4)/dt = [p^*(t) - k^*Z(t)]/m^* \tag{10}$$

The four first-order equations in Eqs. (9) and (10) are then integrated numerically, given the initial conditions for the state vectors Z(i), i = 1 to 4, and an initial integration time step.

A time-step optimization scheme is implemented in DEQS to effectively adjust the step-size within a step for convergence, as well as to reduce the total number of integration steps in the analysis. When a solution does not converge for a prescribed error-bound in a step, the initial step-size is halved and the process is repeated, up to eight times if necessary, until the convergence criterion is satisfied. Once the solution converges, a second test is checked to determine if the step-size can be doubled for the next step. This scheme would effectively result in a time-history solution with variable time-steps.

SELECTION OF DISPLACEMENT SHAPE FUNCTION

The vibrating frequency of an SDOF system is known to have a controlling influence on its dynamic behavior. In addition, it is obvious by inspecting Eqs. (6a) to (6c) and Eq. (7) that the accuracy of the vibrating frequency obtained by Rayleigh's method depends entirely on the shape function P(x), which is assumed to represent the vibration-mode shape. In principal, any shape that satisfies the geometric boundary conditions of the beam may be selected. However, any shape other than the true vibration shape would require the action of additional constraints to maintain equilibrium; these extra constraints would stiffen the system, and thus would cause an increase in the computed frequency. Consequently, it may be recognized that the true vibration shape will yield the lowest frequency obtainable by Rayleigh's method. But,

since the true vibration shape of the CDF mast is not known a priori, a close approximation must be made. The CDF antenna mast resembles a vertical cantilever beam carrying a point mass at its free-end; therefore, the deflection shape of a uniform cantilever beam carrying a point mass at its free-end was chosen as the first approximation to the true vibration shape of the CDF antenna mast arrangement shown in figure 1. This shape function, which was normalized by its tip amplitude, is given by

$$P(x) = (x/L)^2(3/2 - x/2L) \tag{11}$$

in which L represents the length of the mast, from the 010 level up to the tip of the task lamp.

Although the shape function given by Eq. (11) will render a sufficiently accurate vibration frequency for a uniform beam, it is not the true mode shape of the antenna mast that features segmented, partially tapered sections and carries several point masses. An improved procedure is necessary to account for these variations. Reference 1 suggested that using the deflection curve of the beam resulting from the static application of its own weight and the point masses as the mode shape will yield extremely accurate frequency in Rayleigh's procedure. This improved Rayleigh's method is implemented in MASTY as follows:

Consider the elementary theory of a beam in which the curvature of the deflection curve for a beam subjected to the bending moment distribution M(x) caused by its own weight and the point masses it carries can be written in terms of the differential equation

$$d^2y_{st}(x)/dx^2 = -M(x)/EI(x) \tag{12}$$

in which $y_{st}(x)$ represents the lateral deflection of the beam at a point x. Eq. (12) can be integrated once to obtained the slope of the deflection curve and again to obtain the deflection curve, subjected to the following boundary conditions:

$$dy_{st}/dx = 0 \quad \text{at } x = 0$$
$$\text{and} \qquad y_{st} = 0 \quad \text{at } x = 0$$

Therefore, the improved shape function, which is normalized by the tip deflection of the mast y_o, can be written as

$$P(x) = (1/y_o) \iint [-M(x)/EI(x)]dxdx \tag{13}$$

ANALYSIS RESULTS

The validation of frequency prediction by the computer program MASTY is presented first in the analysis results. The dynamic response of the CDF antenna mast assembly subjected to the athwartship motion recorded at the 010 level during the CG-53 shock trials is presented next. Two CDF antenna arrangements are evaluated for shock environment: (1) TACAN

antenna alone and (2) TACAN and JTIDS antennas in combination. The response histories are plotted and shock spectrum analyses are performed with the YADAP code.

VALIDATION OF FREQUENCY PREDICTION BY MASTY

First Example Problem

Two textbook example problems are presented here to validate Rayleigh's procedure implemented in MASTY to compute the fundamental frequency of a vibrating beam. The first example, figure 3, shows a 5-inch OD, 1-inch thick, and 250-inch long uniform aluminum cantilever beam carrying a 50-lb point mass at its free-end. The fundamental frequency of the system is given by the close form solution found on p. 34 of reference 1

$$f_1 = (1/6.2832)\sqrt{3EIg/l^3[W + (33/140)wl]} \qquad (14)$$

in which w is the weight per unit length of the beam of length l, W is the point mass, and g is the gravitational acceleration, i.e., g = 386.4 inch/sec^2. Evaluating the flexural stiffness EI for the aluminum tubing and substituting into Eq. (14), the fundamental frequency of the system is found to be f_1 = 2.0113 Hz.

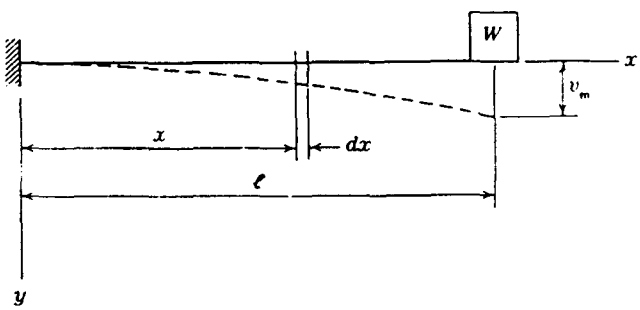

Figure 3. A uniform cantilever beam carrying a point mass at its free-end.

The frequencies computed by MASTY using the shape functions given by Eqs. (11) and (13) are listed in table 1 to compare them with the close form solution given by Eq. (14).

Table 1. Comparison of computed frequency with close form solution for the first example.

Shape Function	Computed Freq.	Close Form Soln.	Percent Error
Eq. (11)	2.0071 Hz	2.0113 Hz	0.208 %
Eq. (13)	2.0025 Hz	2.0113 Hz	0.437 %

As can be seen in table 1, the natural frequencies of the system predicted by the two shape functions are very close, and they are both within 1% of the exact solution given by Eq. (14). That the results shown in table 1 are very accurate is of no surprise because the shape function used in MASTY, i.e., Eq.(11), is the exact deflection shape for the problem considered. The

small discrepency here can be attributed to the error in the numerical integration of the generalized properties given by Eqs. (6a) and (6b). The effect of the improved shape function Eq. (13), which was not realized in this problem, will be demonstrated in the next example.

Second Example Problem

The second example involves the free vibration of a tapered beam fixed at one end, as shown in figure 4. The beam has a unit width, a length l and a depth of 2b at the fixed end. The exact solution, which can be found on p. 467 of reference 1, is

$$f_1 = (5.315b/6.2832l^2)\sqrt{E/(3r)} \tag{15}$$

in which E is the Young's modulus, and r is the mass density.

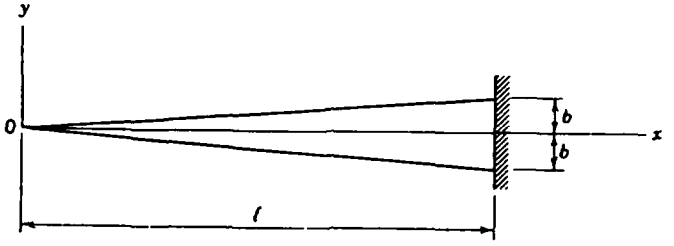

Figure 4. A tapered cantilever beam of unit width.

Let $l = 30.4$ inches $\quad b = 1$ inch
$E = 10 \times 10^6$ psi $\quad r = 0.2588 \times 10^{-3}$ lb-sec^2/in^4

and the natural frequency of the tapered beam is $f_1 = 103.88$ Hz.

The frequencies computed by MASTY using the first approximation and the improved shape function are compared with the exact solution and are given in table 2.

Table 2. Comparison of computed frequency with close form solution for the second example.

Shape Function	Computed Freq.	Close Form Soln.	Percent Error
Eq. (11)	113.71 Hz	103.88 Hz	9.45 %
Eq. (13)	106.06 Hz	103.88 Hz	2.10 %

As shown in table 2, using the deflection shape of the uniform beam, Eq. (11), to approximate the mode shape of the tapered beam would result in a 9.45% error in the natural frequency prediction for this example. Table 2 also shows that the calculated frequency improves dramatically with the use of the improved shape function Eq. (13), which is the static deflection curve of the beam derived in the program that was based upon the actual weight and stiffness distributions of the beam.

It can be concluded that, in order to improve the accuracy in the natural frequency prediction and in the follow-on response calculation for the antenna mast subjected to base motion, the static deflection curve of the mast due to its own weight and the attached masses it carries shall be derived and used as the mode shape of vibration.

DYNAMIC RESPONSE OF THE CDF ANTENNA MAST TO BASE MOTION

The Antenna Mast Models

The cantilever beam model of the antenna mast assembly programmed in MASTY includes four segments of antenna mast above the 010 level. They are the pole mast, vertical CDF mast, the extender tube, and the task lamp assembly, as shown in figure. Except for the CDF vertical mast that has nonuniform cross sections, all others are of uniform cross sections. Since the only drawings available at the time when this analysis was performed were the outline and installation drawings for the CDF and TACAN antennas (references 6 and 7, respectively), the key dimensions of the vertical mast, such as the ODs and wall thicknesses, were not available. These dimensions were obtained using the ultrasonic measurement of a Version-1 CDF vertical mast for a DDG 72 mast mock-up of the 010 level and above, which was being tested at the antenna range at NRaD. The measurements were conducted by Code 815, and the results were reported in reference 8. These measured data were used in the analysis in lieu of the dimensions given by the engineering drawings. Figure 5 shows the cross section view of the CDF vertical mast model constructed with the measured data.

The antenna assemblies, including three UHFs on the pole mast, the CDF and the dipole antennas on the vertical mast, and the TACAN and the JTIDS atop the task lamp, are modeled as lumped masses, and they are attached to their respective center of gravity (CG) locations on the mast. Contrary to the flexible mast segments, rigid connections are assumed between the TACAN and the JTIDS and between the JTIDS and the task lamp. The two heat sinks on the CDF vertical mast are also modeled as lumped masses. Two antenna mast models are created, the one with TACAN antenna only atop the task lamp and the other with TACAN and JTIDS antennas in series. The models are fixed at the base of the pole mast, at which the base-motion induced by a near-miss underwater explosion is to be applied.

Idealized Ship Shock Input

An idealized shock input that simulates the athwartship component (y-direction) of the shock response data recorded at the 010 level during a CG 53 shock trial is given in figure 6a. As shown, the 4-Hz sinusoidal motion has an amplitude of 8 g, and the motion maintains its full amplitude for 1 second (4 cycles) before diminishing to zero in about 3 seconds. This idealization is based on a description of shipboard shock in a Naval Research Laboratory technical report (reference 9), which states that a typical acceleration waveform found in shipboard shock would remain significant for about 1 second. Figure 6b shows the shock spectrum of the input motion.

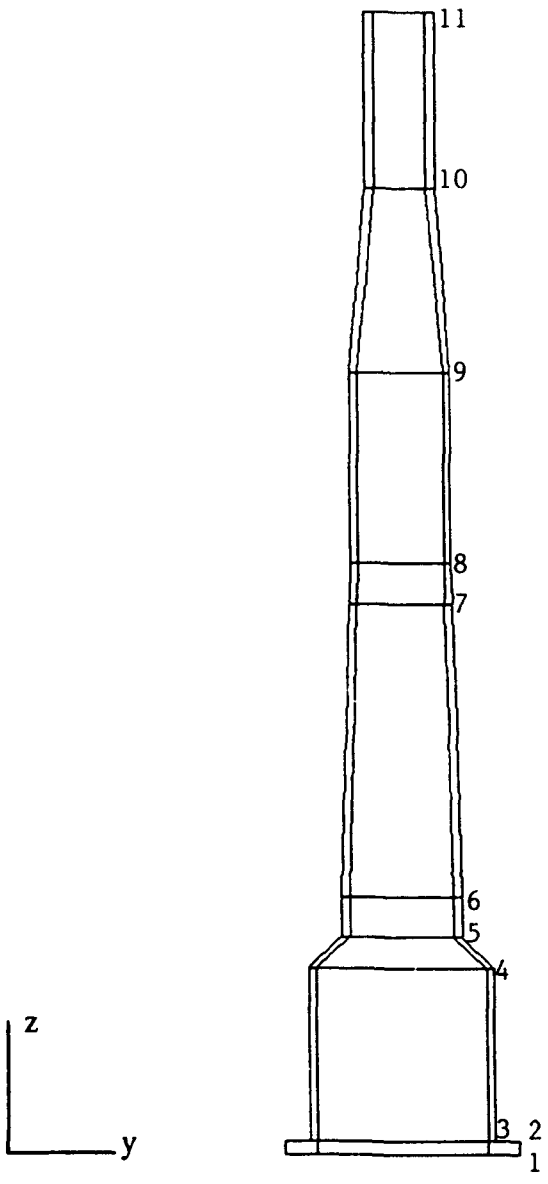

Mast Location	Z-axis (in)	OD (in)	Thickness (in)
11	84.0	5.093	0.734
10	71.0	5.093	0.734
9	57.5	7.202	0.477
8	43.5	7.202	0.468
7	40.5	7.480	0.599
6	19.0	8.753	0.614
5	16.0	8.753	0.614
4	13.75	13.528	0.795
3	1.0	13.528	0.795
2	1.0	17.189	2.376
1	0.0	17.189	2.376

Figure 5. Longitudinal section of the CDF antenna mast model.

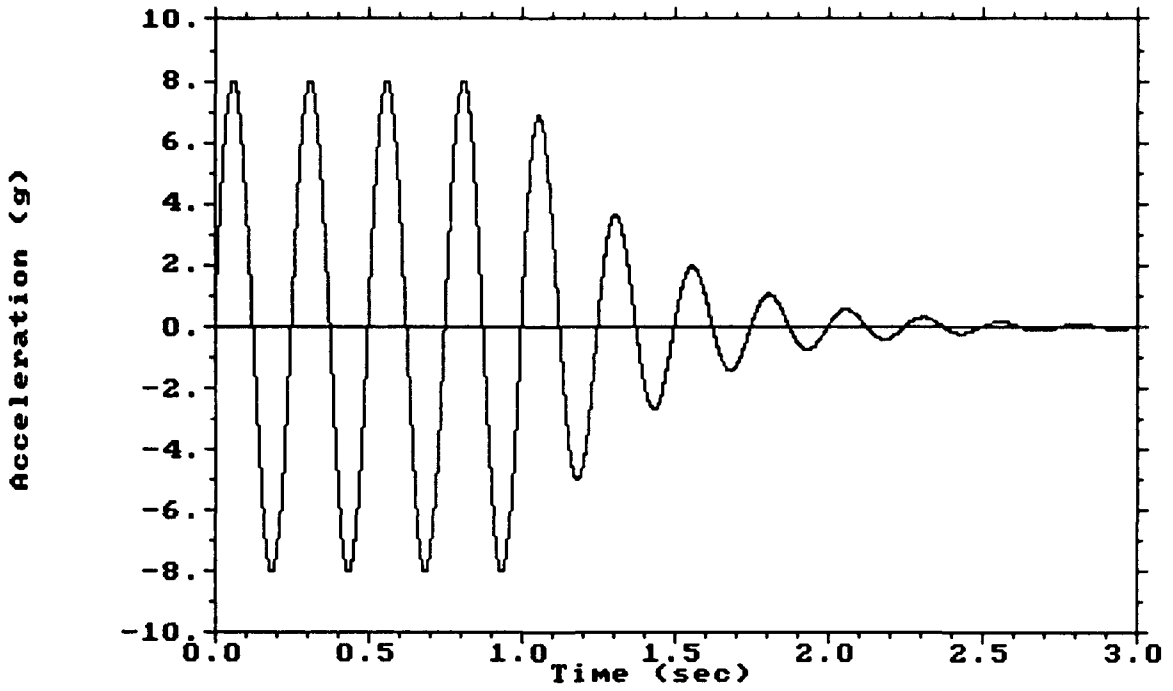

Figure 6a. Idealized acceleration waveform of shipboard shock at the 010 level.

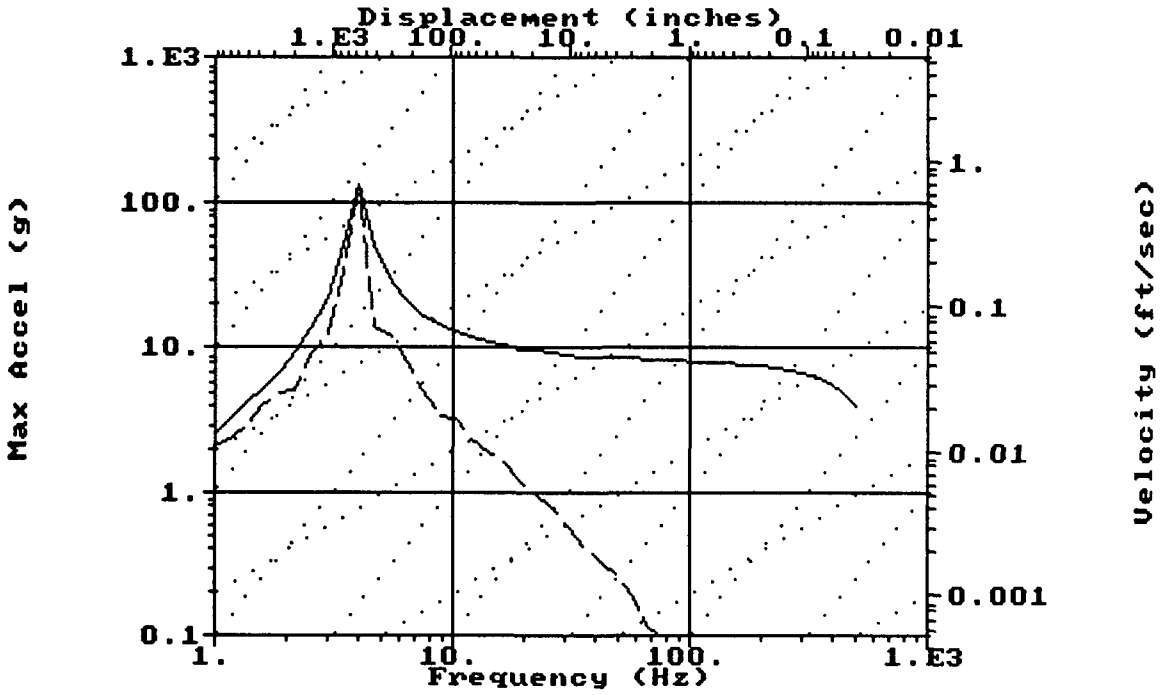

Figure 6b. Shock spectrum of the idealized acceleration waveform.

Output of MASTY Computer Runs

The output of MASTY computer runs for the two CDF antenna mast models subjected to the base motion shown in figure 6a are listed in appendices A and B, respectively. Part I of the output tabulates the physical properties of the antenna mast components, including the weights of the antennas and the heat sink units, their CG locations on the mast, and the lengths and flexural stiffnesses of the mast segments. The rotary inertia of the components, which were accounted for in the formulation, were ignored in the current analyses. Part I also lists the input data for the ODs and thicknesses at several discrete locations on the CDF vertical mast to define its variable cross sections. Note that these locations, which are marked on the vertical mast model shown in figure 5, correspond to the locations where the ultrasonic measurements of a CDF vertical mast mock-up were taken and that the computer program was written so that the ODs and the thicknesses vary linearly between any two discrete points. This permits the tapered beams to be modeled precisely in the program.

Part II lists the material properties of the antenna mast segments, including Young's moduli, Poisson's ratios, densities, yield, and and ultimate strengths of the material. The section moduli of the mast segments, including those at the base of the CDF mast, are also listed in Part II.

Part III shows the generalized properties and the fundamental frequency of the idealized SDOF antenna mast system that were computed using the static deflection curve of the mast due to its own weight and attached masses it carries as the mode shape. The contributions to the generalized mass by the distributed structural mass, the point mass, and the rotary inertia are also given in Part III.

Part IV lists the initial and final integration information on the step-size and the local truncation error of the predicted state vector, which is used in the program as a measure to vary the step-size in the variable-stepped numerical integration procedure. Messages will be given here if the integration fails to converge in a step when (1) the number of times the step-size is halved to repeat the integration exceeds eight, or (2) the last halved step-size exceeds the pre-specified allowable minimum. This information will provide clues to either loosen the error-bound for convergence or increase the number of consecutive times the step-size can be halved before repeating the time integration. Note that a looser error-bound will result in a less accurate numerical solution.

Part V tabulates the maximum and minimum values of the selected dynamic response variables at the specific locations on the mast. The response variables listed in Part V include the translational and rotational displacements and accelerations at the TACAN and JTIDS antennas, which undergo maximum motions in the fundamental mode. Because of the rigid connections assumed between TACAN and JTIDS and between JTIDS and the tip of the task lamp, the rotations at the TACAN and JTIDS are identical to that of the tip of the task lamp. The motion-induced shear forces and bending moments along the length of the mast are given

in Part VI, including those at the bases of the pole mast, the CDF mast, and the extender tube, which is considered to be the weakest link in the whole mast. The maximum and minimum flexural stresses, which occur at the outmost fibers of the mast's cross sections at these critical locations, are also given in Part IV. The entire time-histories of the response variables are saved in TAPE9 for plotting and response spectrum analyses with YADAP. A TAPE9 plot file, with response variables written every 10 time steps, is listed in appendix C.

Dynamic Responses of the CDF Antenna Mast without JTIDS

Figures 7a and 7b show plots of the TACAN antenna's displacement- and acceleration-time histories, responding to the 8-g/4-Hz athwartship shock for the CDF antenna mast without the JTIDS. In general, a forced vibration is a superposition of some free vibrations of the system and a steady-state vibration maintained by the disturbing force. Figure 7a shows that the 4-Hz base motion forces the TACAN antenna to oscillate with an amplitude that rises, peaks, and falls within about 1 second. The peak amplitudes in this period are 25.4-inch displacement, 51.5-g acceleartion, and 11.4° rotation. But, the motion settles down to a free vibration of 20 g and 4.96 Hz after roughly 2.5 seconds when the excitation diminishes. However, it is rather difficult to visualize the content of the two frequencies in the forced vibration phase of the time-history plots shown in figures 7a and 7b. The response shock spectrum shown in figure 7c serves its purpose here as it clearly indicates the participation of the two frequencies in the forced vibration phase of the response motion for the TACAN antenna. During this phase, the shear force and the bending moment at the base of the extender tube reach their respective maximum values of -7,393 lb and -361,700 in-lb, as shown in figures 8a and 8b. The corresponding flexural stress is 69,709 psi, which results in a margin of safety (MS) of -0.053. The MS is defined as

$$\text{MS} = (\text{ultimate strength/max stress}) - 1 \qquad (16)$$

in which the ultimate strength (ULT) of the material is taken to be the same as that under a static loading condition, i.e., ULT = 66,000 psi for the 7075-T73 aluminum. It is known that the tensile strength of material generally increases when the strain rate increases. Therefore, it is conservative to assume that the ULT under a dynamic loading condition is the same as that under a static loading condition. The maximum flexural stress in Eq. (16) is obtained by dividing the maximum bending moment at the base of the extender tube by its section modulus given in appendix A. A small negative MS of -0.053 means that the extender tube is on the borderline of being able to sustain the shock. The maximum bending moment at the base of the pole mast is 2,960,100 in-lb, which results in a maximum flexural stress of 33,336 psi and a safe MS of 0.98.

It is interesting to point out that had the full amplitude of the excitation lasted longer than 1 second, say 2 seconds as shown in figure 9a, the rise and fall motion between 0 and 1 second shown in figures 7a and 7b, would have repeated itself before settling down to the free vibration, as shown in figure 9b. This kind of vibration that builds up and diminishes in a

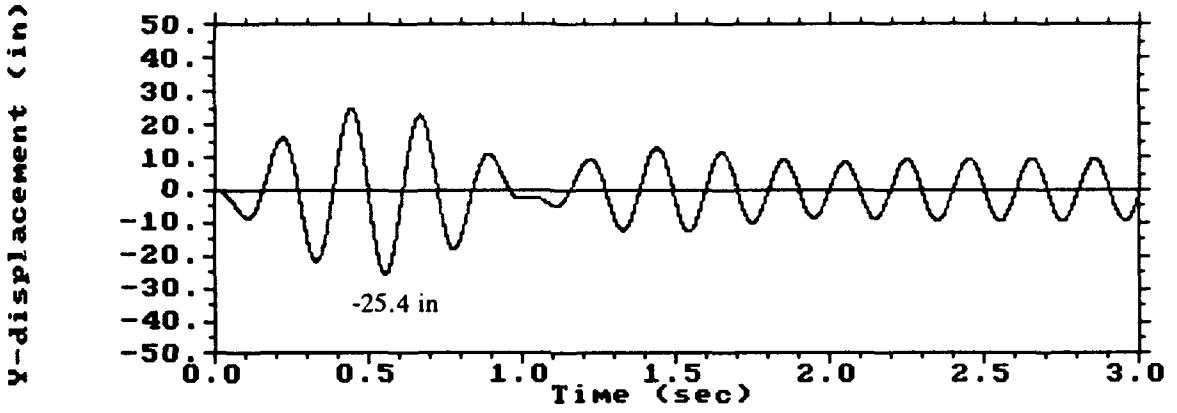

Figure 7a. Displacement history of TACAN antenna (without JTIDS) due to 4-Hz shipboard shock.

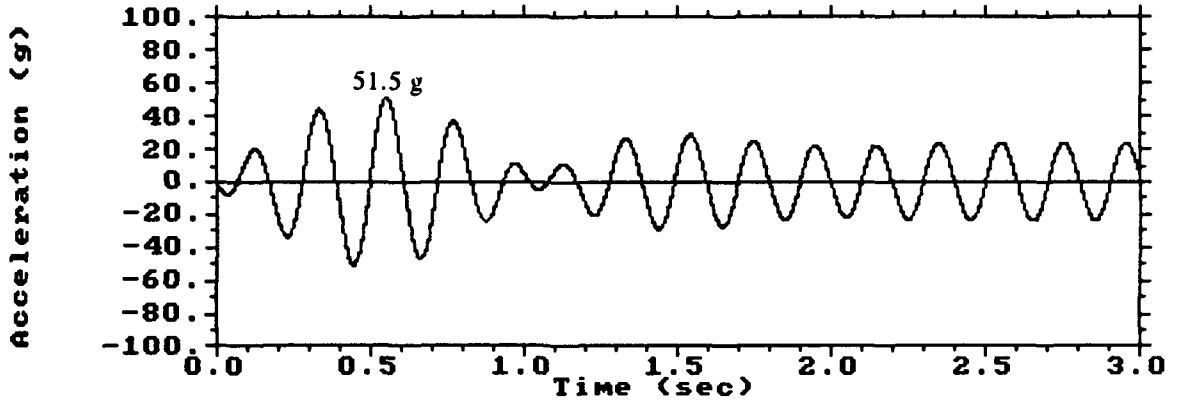

Figure 7b. Acceleration history of TACAN antenna (without JTIDS) due to 4-Hz shipboard shock.

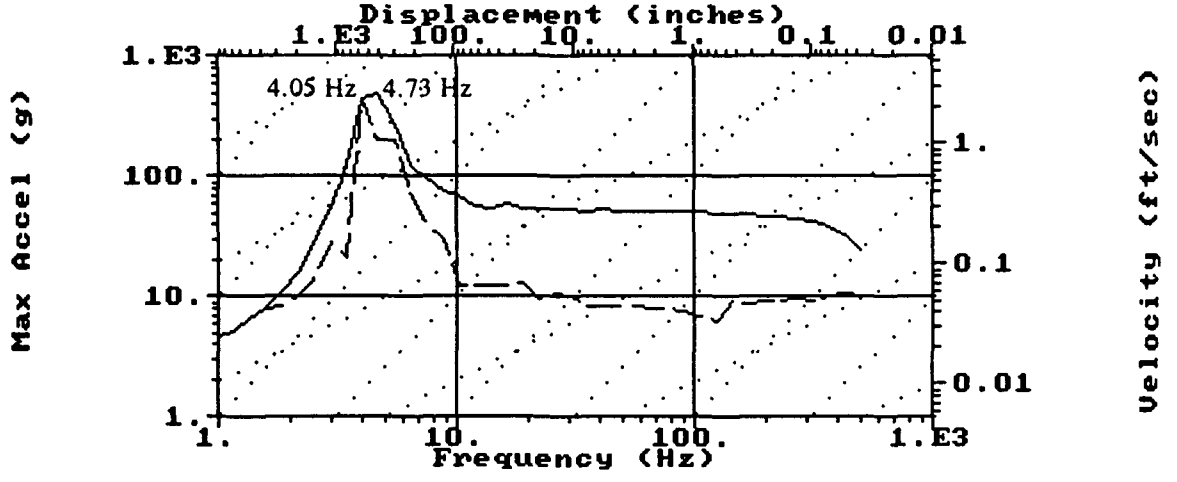

Figure 7c. Response spectrum of TACAN antenna (without JTIDS) due to 4-Hz shipboard shock.

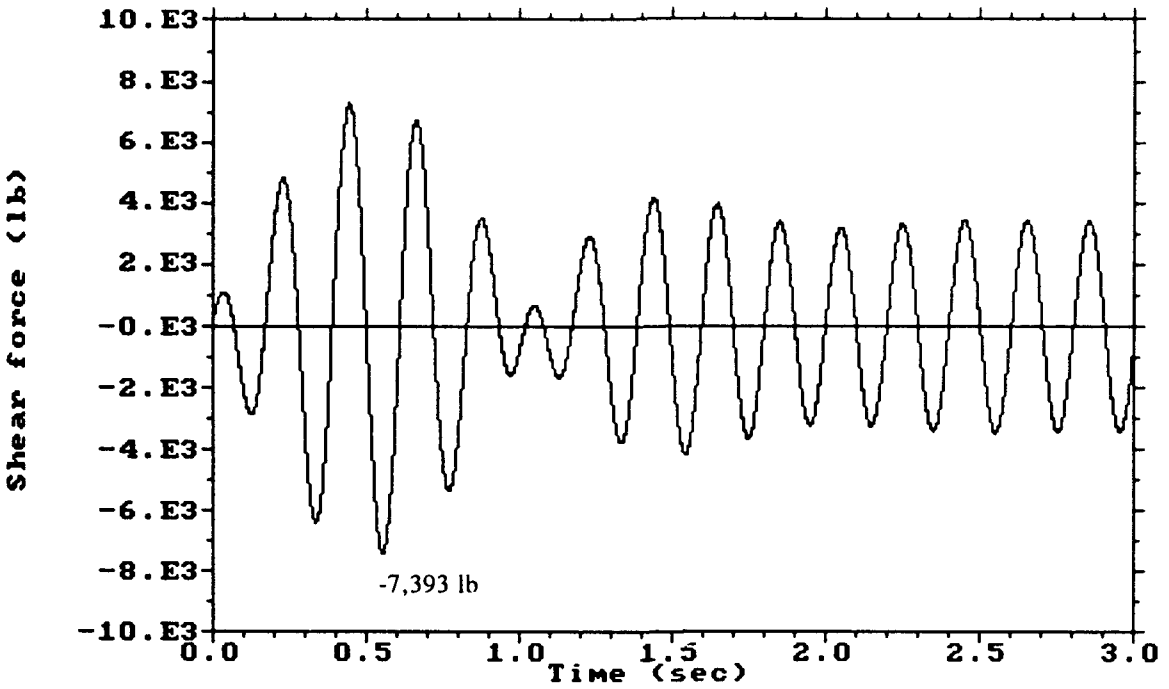

Figure 8a. Shear force history at base of extender tube (without JTIDS) due to 4-Hz shipboard shock.

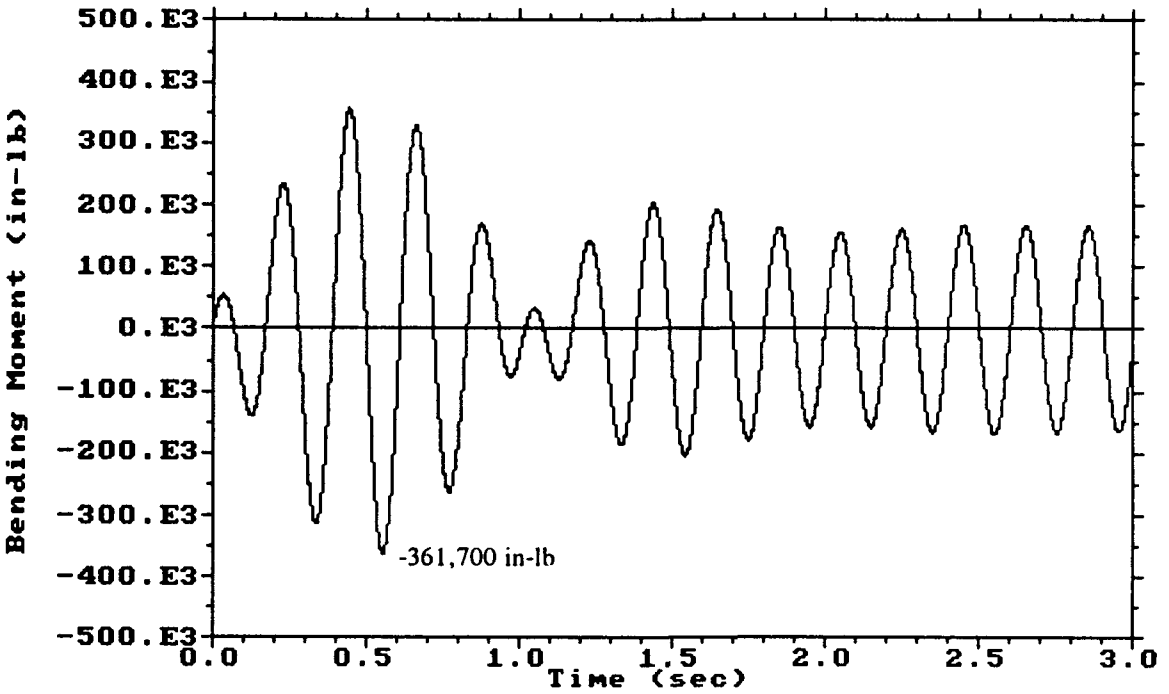

Figure 8b. Bending moment history at base of extender tube (without JTIDS) due to 4-Hz shipboard shock.

regular pattern of beats is known as "beating" in forced vibration, which happens when the drive frequency is close to the natural frequency of the system, as is the case here. The period of "beating," which depends on how close the two frequencies are, can be approximated by the equation

$$T_b = 1/(f_n - f) = 1.042 \text{ second}$$

in which f_n and f are the natural frequency of the system and the driving frequency of the base motion, respectively. This period of beating of slightly over 1 second can be clearly observed in figure 9b.

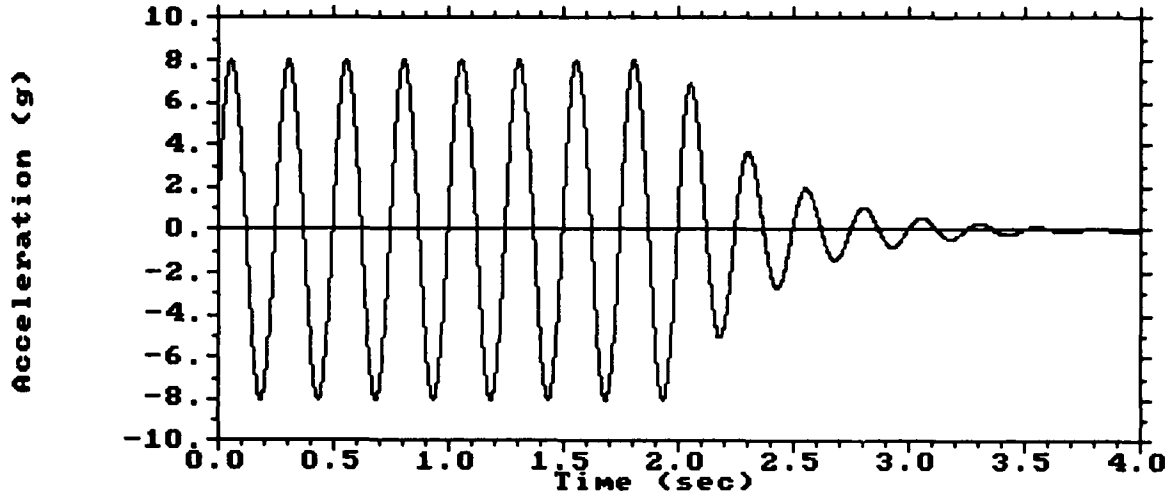

Figure 9a. Idealized input acceleration waveform with a 2-second duration of peak amplitude.

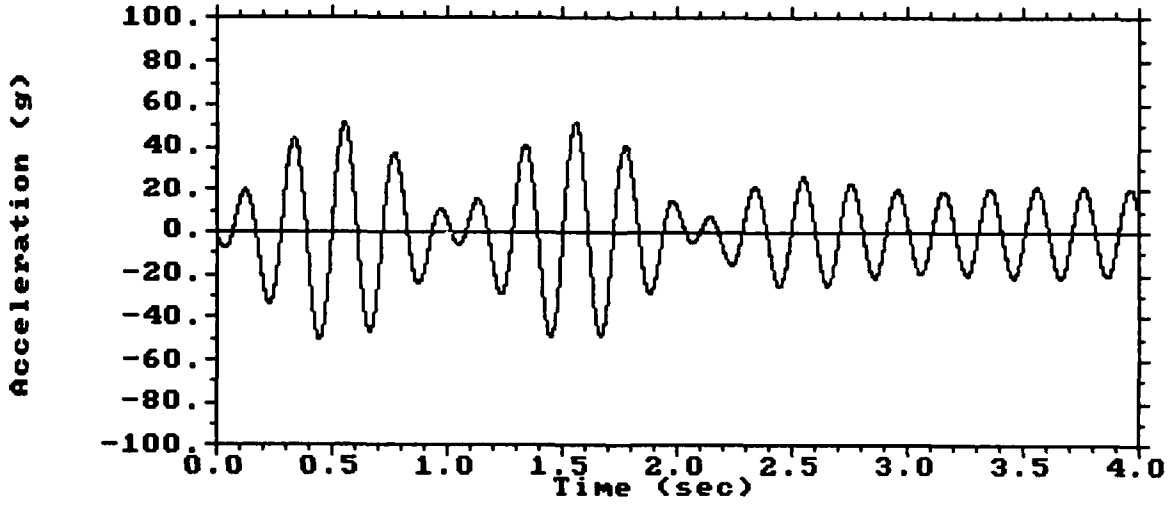

Figure 9b. Displacement history of TACAN antenna showing a "beating" pattern during the forced vibration phase of the response motion.

Dynamic Responses of the CDF Antenna Mast with JTIDS

With both TACAN and JTIDS antennas atop the CDF mast, the natural frequency f the system reduces from 4.96 Hz to 3.25 Hz, as shown in appendix B. The displacement- and acceleration-time histories of the TACAN antenna are plotted in figures 10a and 10b, respectively, while the time histories of the shear force and bending moment at the base of the extender tube are plotted in figures 11a and 11b, respectively. With the natural frequency of the system (3.25 Hz) now closer to the 4-Hz drive frequency of the excitation than the one with TACAN alone (4.96 Hz), the system vibrates in the similar "beating" pattern, but with a longer period (T_b = 1.333 second) and greater amplitudes and reacts with higher internal loads. The maximum responses at the TACAN are 46-inch deflection, 61.1-g acceleration, and 19.6° rotation. The maximum shear force and bending moment at the base of the extender tube increase to -14,819 lb and -967,610 in-lb, respectively. The maximum flexural stress is 186,480 psi, which is high above the ULT of the material and results in a high negative MS of -0.65. This means the extender tube would definitely fail under such a high-stress condition.

Analysis results given in appendix B also indicate that the flexural stresses are quite high at the CDF antenna location on the vertical mast and at the base of the pole mast. The maximum stress at the CDF antenna location is 62,718 psi for a marginal MS of 0.052, while the maximum stress at the base of the pole mast is 56,490 psi for a low MS of 0.168. These results suggest that these locations are vulnerable to potential failure.

Vibration Mode Shape of the CDF Antenna Mast

As described earlier, in order to improve the accuracy of the vibration analysis using Rayleigh's method, the static deflection curve of the mast due to its own weight distribution and the attached masses it carried was derived in MASTY and was used as the mode shape in lieu of the first approximation. Recall that the first approximation mode shape was based on the deflection shape of a uniform beam carrying an end mass. To ensure that the improvement was indeed made here, the natural frequencies of the antenna mast assembly supporting TACAN and JTIDS calculated with both mode shapes (4.13 Hz with the first approximation and 3.25 Hz with the improved mode shape) are compared with the prediction made in a separate finite element analysis using MSC/PAL-II* (3.19 Hz). The discrepencies are +29.47% for the former and +1.88% for the latter. The improvement made by the improved mode shape over the first approximation is quite significant. The mode shapes for both methods are plotted in figure 12, and they show that the first approximation mode shape clearly overestimates the flexural stiffness of the mast as it bends much less over the area of the mast occupied by the flexible extender tube (222-inch to 253-inch station). Note that both mode shapes are normalized by the amplitude at the tip of the task lamp (at the 264-inch station). Overestimation of the flexural stiffness would result in a higher natural frequency prediction for the antenna mast, as indicated in figure 12.

* MSC/PAL-II is an FEA computer code that is the registered trademark of MacNeal/Schwendler Corporation.

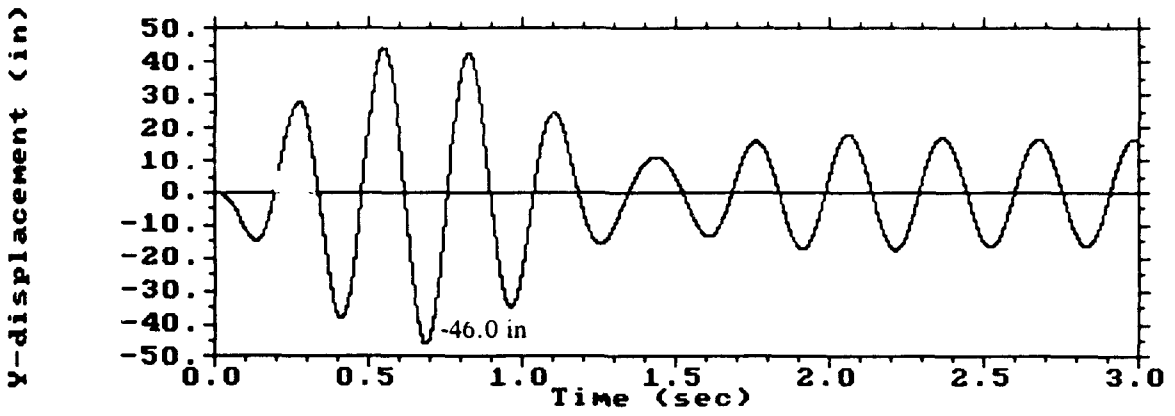

Figure 10a. Displacement history of TACAN antenna (with JTIDS) due to 4-Hz shipboard shock.

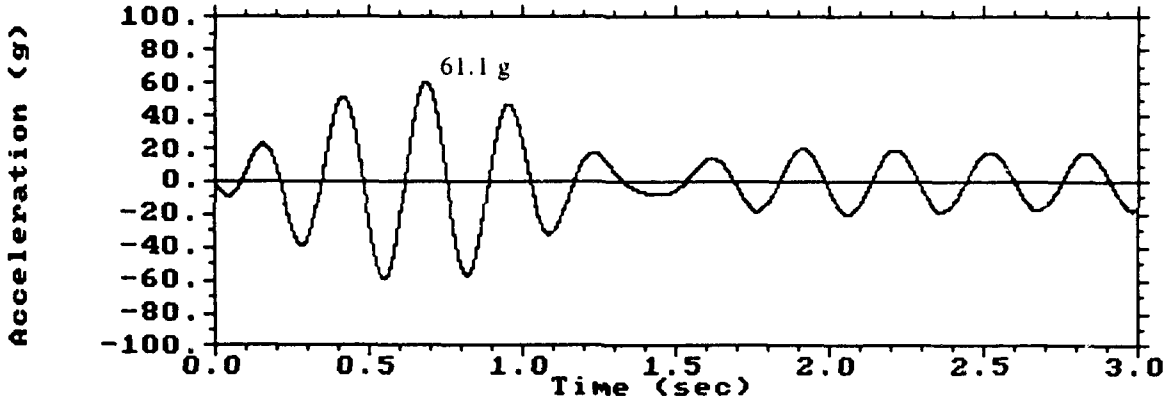

Figure 10b. Acceleration history of TACAN antenna (with JTIDS) due to 4-Hz shipboard shock.

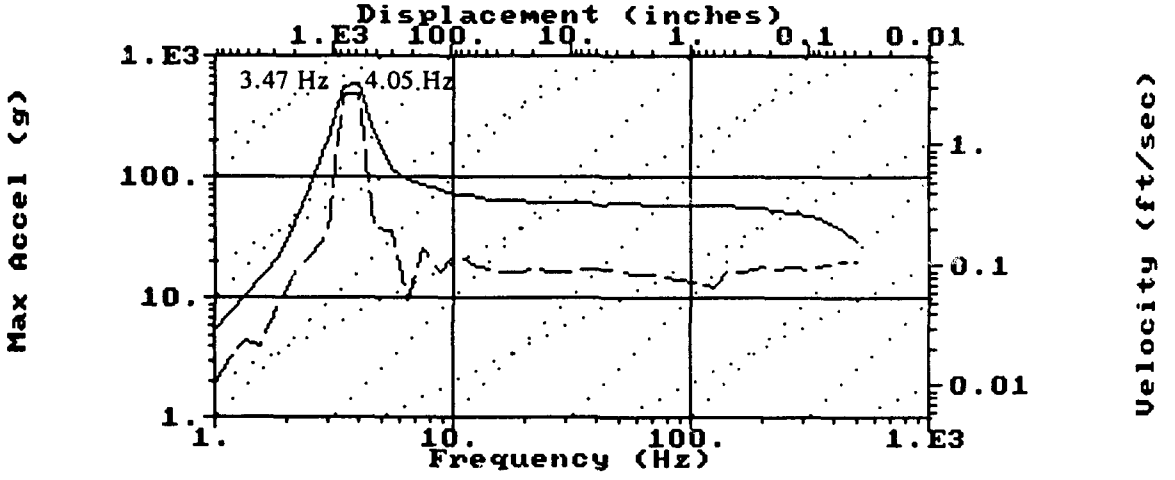

Figure 10c. Response spectrum of TACAN antenna (with JTIDS) due to 4-Hz shipboard shock.

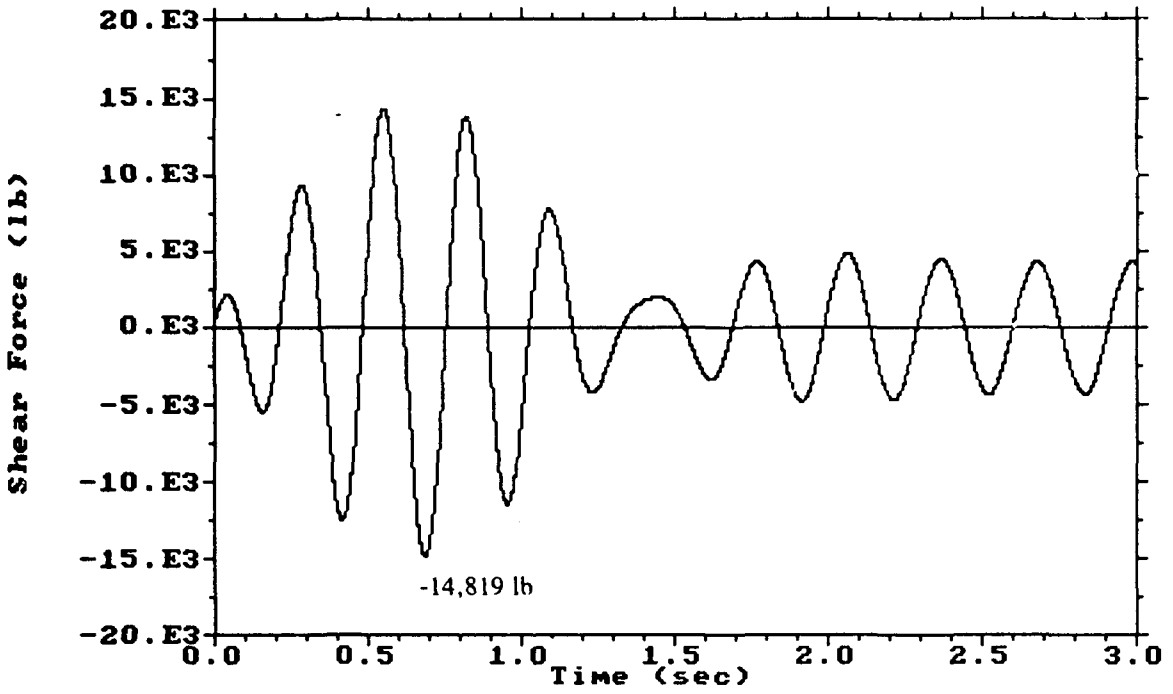

Figure 11a. Shear force history at base of extender tube (with JTIDS) due to 4-Hz shipboard shock.

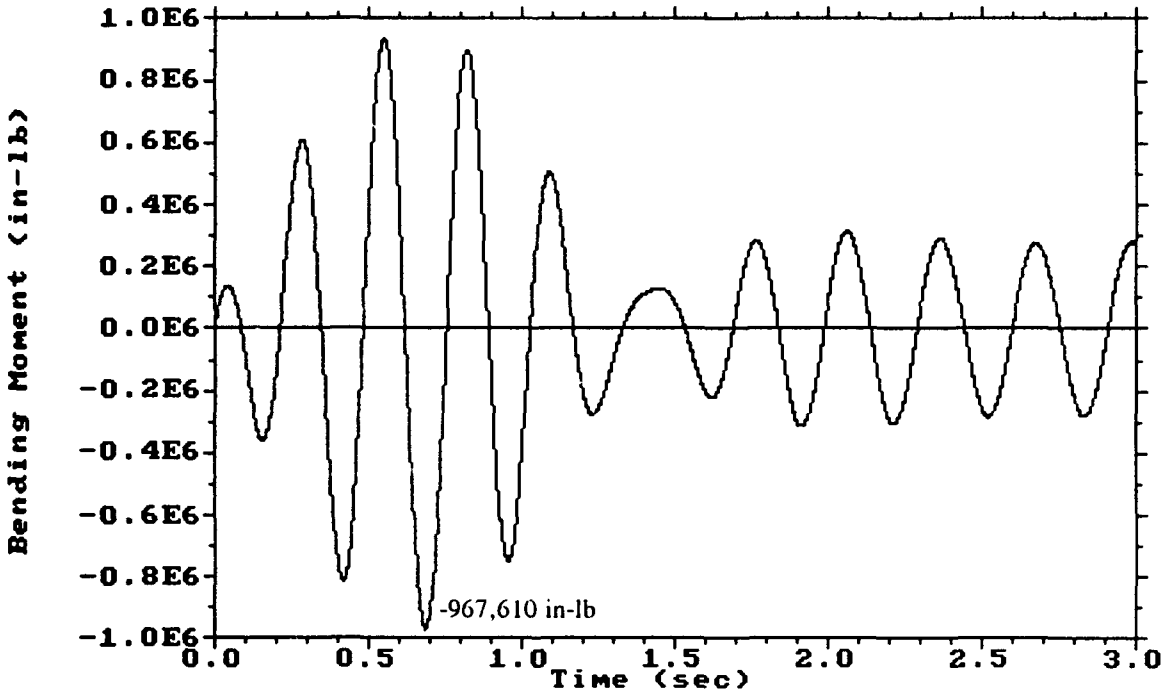

Figure 11b. Bending moment history at base of extender tube (with JTIDS) due to 4-Hz shipboard shock.

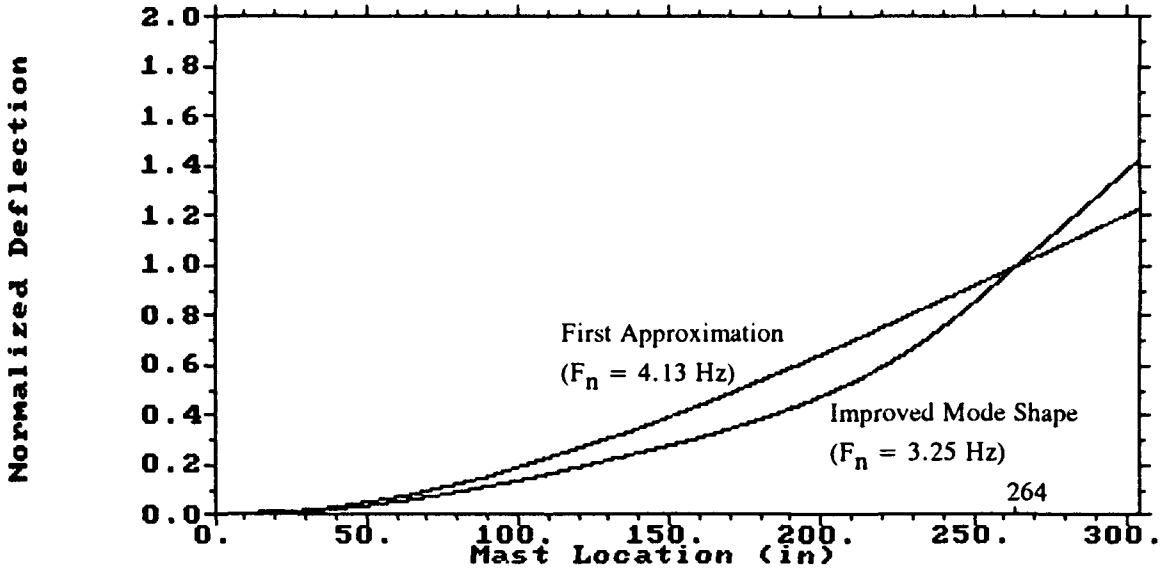

Figure 12. First approximation mode shape versus improved mode shape.

SUMMARY AND CONCLUSIONS

The envelopes of maximum shear force and bending moment distributions for the two antenna mast arrangements subjected to the 8-g/4-Hz idealized athwartship shock, are given in figures 13a and 13b, respectively. As shown, the extra weight at the tip of the mast and a higher resulting motion cause the mast that carries both TACAN and JTIDS to react with higher shear forces and bending moments along the entire length of the mast. As a result, high stresses are encountered at several critical locations on the mast, including the base of the extender tube, which is considered to be most critical.

Table 3 summarizes the dynamic responses of the two antenna mast arrangements. It indicates that, under the shipboard shock environment considered, the modified Version-1 CDF antenna mast assembly with a Version-2 extender tube (4.615-inch OD and 0.403-inch thick) is barely able to support the TACAN antenna alone. But, it cannot support both TACAN and JTIDS antennas in combination because of the excessive bending stress developed at the base of the extender tube by the shipboard shock.

Table 3. Summary of dynamic responses for two CDF antenna mast arrangements.

Antenna Arrangement	Natural Frequency	Athwartship Shock Input	Max TACAN Response	At Base of Ext Tube Shear	Moment	Stress	Safety Margin
			Disp/Accel/Rotation	(lb)	(in-lb)	(psi)	
TACAN Alone	4.96 Hz	8 g/4 Hz	25.4"/51.5 g/11.4°	7,393	361,700	69,709	-0.05
TACAN/JTIDS	3.25 Hz	8 g/4 Hz	46.0"/61.1 g/19.6°	14,819	967,610	186,473	-0.65

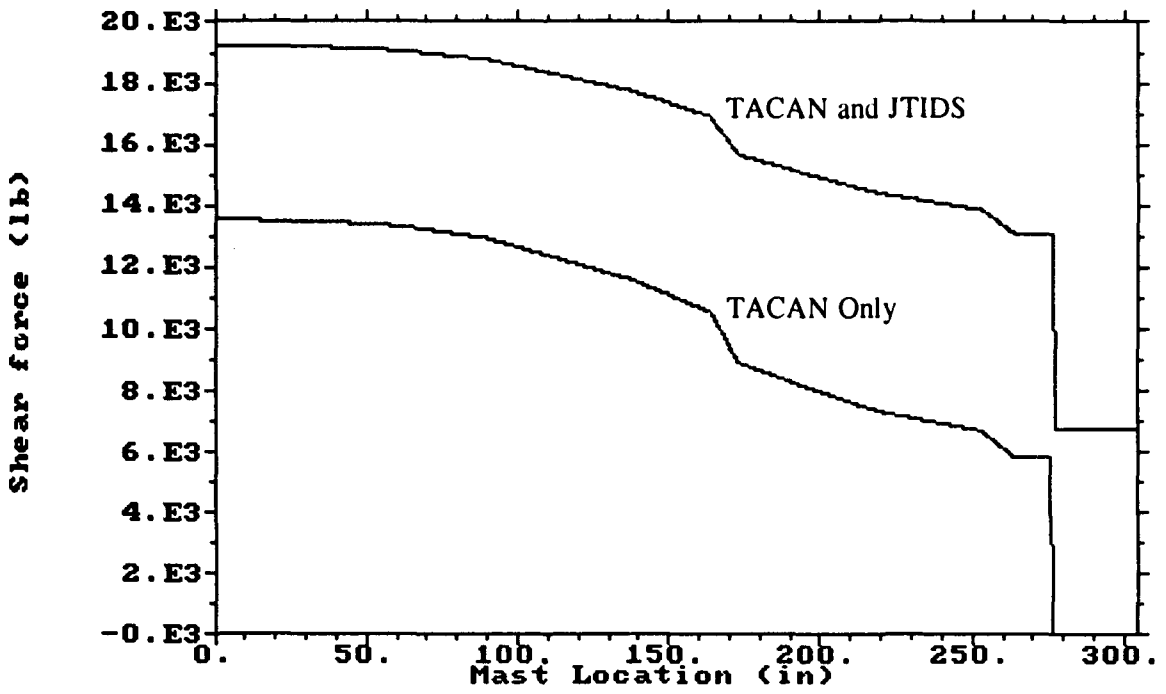

Figure 13a. Envelopes of maximum shear force distributions for two antenna mast arrangements due to 4-Hz shipboard shock.

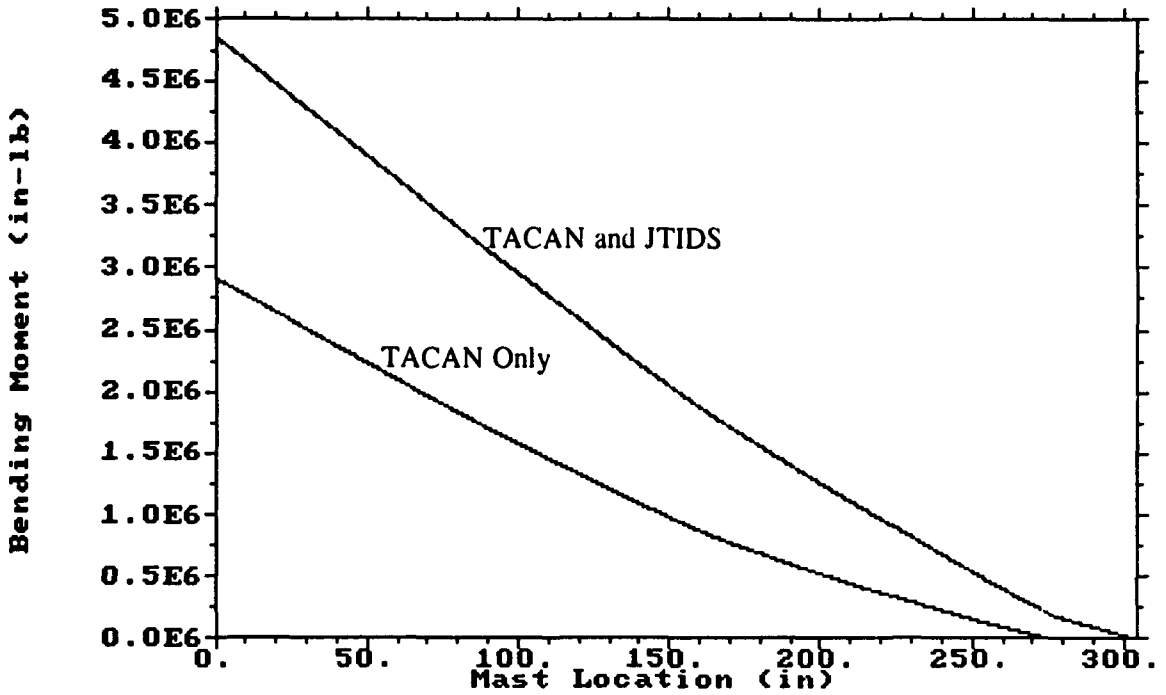

Figure 13b. Envelopes of maximum bending moment distributions for two antenna mast arrangements due to 4-Hz shipboard shock.

DISCUSSION AND RECOMMENDATIONS

The steady-state response for the forced vibration of an undamped SDOF system subjected to base motion can be generalized in figure 14. Figure 14 plots the ratio of the relative displacement (y_1-y_o) of the tip mass M to the absolute displacement of the base y_o as a function of the forcing frequency to natural frequency ratio (f/f_n). Three important points can be made about figure 14:

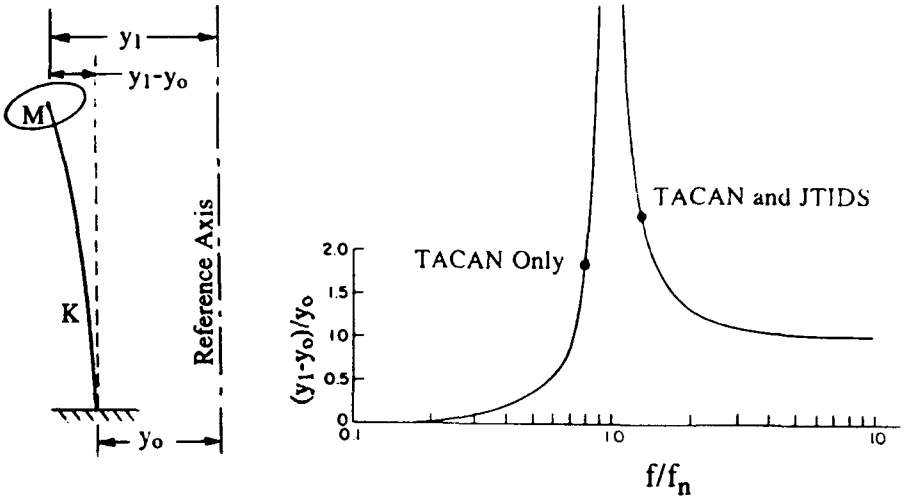

Figure 14. A single-degree-of-freedom system and its response to base motion.

1. When the forcing frequency equals to the natural frequency of the system, i.e., $f/f_n = 1$, resonance occurs, and the response approaches infinity.

2. In the region $f/f_n < 0.6$, where the relative displacement is small and proportional to the acceleration of the base, the system behaves as an accelerometer and serves as the pickup for the base motion.

3. In the region $f/f_n > 2$, where the relative displacement is essentially the same as the absolute displacement of the base, the system is said to be seismically suspended, which means the system is on a soft mount and can be whipping at the same amplitude as the base motion.

The frequency ratios for two antenna mast models analyzed for the 4-Hz base motion are 0.806 for the one with TACAN alone and 1.231 for the other with both TACAN and JTIDS. They are plotted in figure 14, which shows that they both are in an undesirable region of being too close to the disastrous resonance condition. Certainly, strengthening the mast to raise its natural frequency above a specific vaiue, be it 4 Hz, 5 Hz or any value above, is a solution to the problem. One may argue that softening the mast at the other end of the spectrum may offer a solution as well. But, the question arises as to whether the antennas on the mast, especially TACAN and JTIDS, can function properly or withstand the high inertia loads when the soft mast begins to whip. This leaves very little alternative but to strengthen the mast.

A parametric study was performed in an attempt to raise the fundamental frequency of the system (with TACAN and JTIDS) by varying the thickness and/or OD of the extender tube. The results of the study are summarized in table 4. Table 4 shows that replacing the extender tube with a solid rod of the same OD can raise the natural frequency of the system by only 2.06%, while doubling both the OD and the thickness of the extender tube by only 5.45%. Obviously, changing the design of the extender tube alone is not an effective means of raising the natural frequency of the system. Better weight and stiffness distributions of the whole mast are required. The most effective way would be to perform a design optimization for the entire antenna mast assembly to arrive at a minimum weight design that meets a lower bound constraint on the fundamental frequency. This goal can be achieved via the "optimality criteria approach" (reference 10) or by a "numerical search method" (reference 11). In the "optimality criteria approach," a criterion related to the behavior of the structure, such as the fundamental frequency in this case, is derived, and the premise is that when the structure is sized to satisfy this criterion, the merit function (structural weight) automatically attains an optimal value. This approach is strongly recommended here.

Table 4. Sensitivity of the system's fundamental frequency to a design change in the extender tube.

Design Variation	OD/Thk (in/in)	Wt (lb)	EI/L^3 (lb/in)	System's Freq (Hz)	Percent Increase
Current Design	4.615/0.403	16.04	6.486	3.247	
Solid Rod	4.615/2.307	50.30	12.102	3.314	+2.06
Double OD & Thk	9.230/0.806	64.14	103.776	3.424	+5.45

The computer program MASTY developed for this study has provided an effective tool to analyze the dynamic behavior of the antenna mast assembly when subjected to shipboard shock. The important capabilities implemented in the program are

1. the capability to analyze an antenna mast that is composed of a mixture of beam segments with different types of cross sections (circular or rectangular, straight or tapered),

2. the capability to provide an algorithm to derive the static deflection curve of the mast based on its actual weight distribution and the attached masses it carries, and use this curve as the mode shape to derive the natural frequency of the system very accurately,

3. the capability to provide an efficient time-integration routine with a step-size optimizer for the numerical solution to the system's equations of motions, and

4. the capability to provide an output compatible with YADAP code so that the time-histories of the response variables and their shock spectra can be plotted on a PC.

A simplified flow diagram of MASTY is depicted in figure 15. The current version of MASTY, however, can analyze the dynamic behavior of the mast in the athwartship direction (y-direction) only. It can be expanded to analyze the responses in the other two directions, i.e., the forward (x-direction) and the vertical (z-direction) motions.

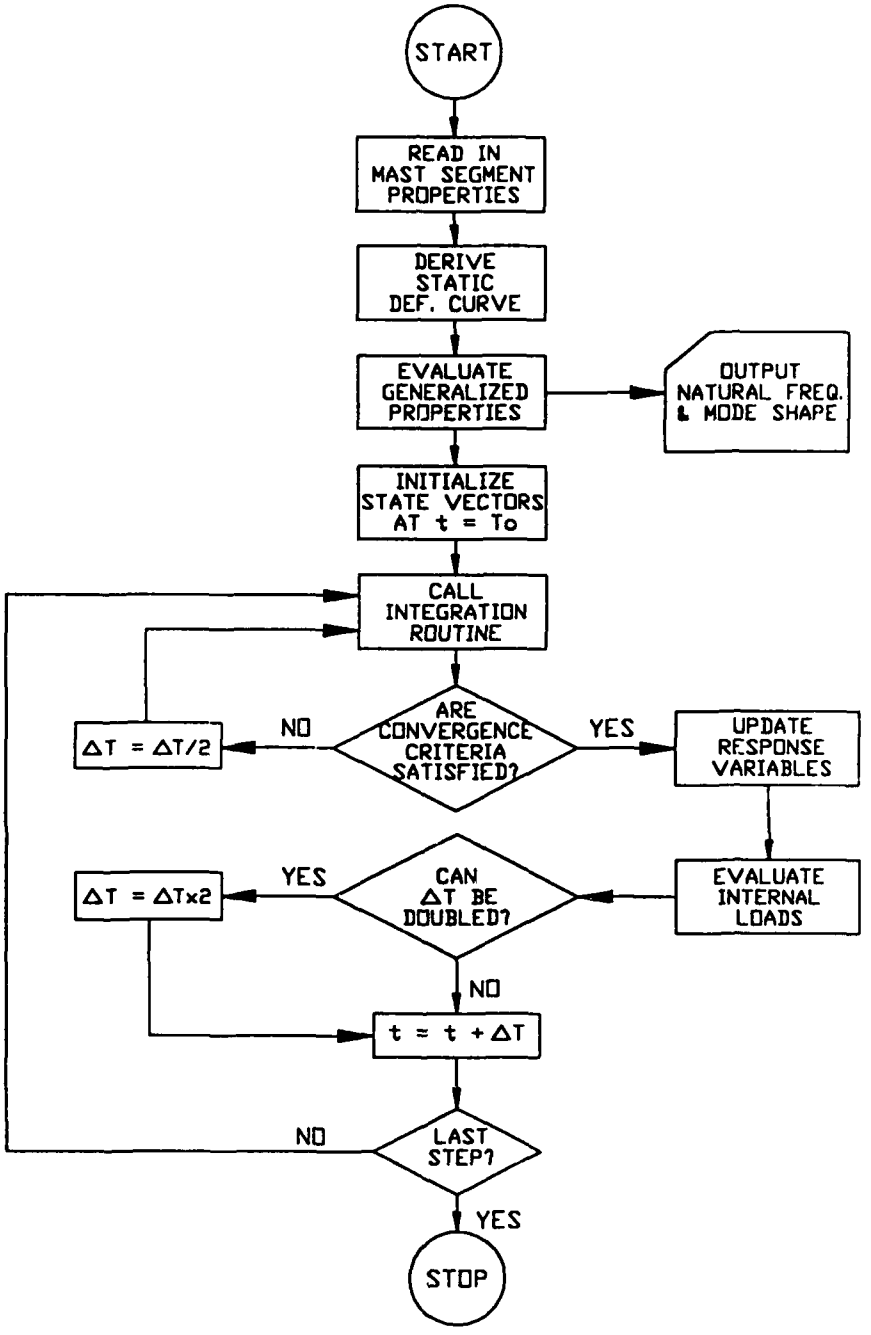

Figure 15. A simplified flow diagram of MASTY.

REFERENCES

1. Timoshenko, S. P., D. H. Young, and W. Weaver, Jr. 1974. "Vibration Problems in Engineering," John Wiley & Sons, Inc., New York, 4th Edition, pp. 31-48.

2. Lambert, J. D. 1973. "Computational Method in Ordinary Differential Equations," John Wiley & Sons, Inc., New York, pp. 120-135.

3. YADAP, a PC computer code developed by D. Worth. Naval Surface Warfare Center, Dahlgren Division Detachment at White Oak, Silver Spring, MD.

4. Shaw, R. C. 1982. "DEQS--A FORTRAN Computer Program for Solving a System of Differential Equations," TRW Interoffice Correspondence 82.H321.4-121.

5. Chalmers, R. H. and R. C. Shaw. 1988. "Using Tuned Fixture to Tailor MIL-S-901C," Conference Proceeding of the 59th Shock and Vibration Symposium, Vol. V, pp. 129-162.

6. Antenna Assembly AS-3506A/SRS-1 Outline and Installation Drawing. 1990. Southwest Research Institute Drawing No. 1133-1011, Southwest Research Institute, San Antonio, TX.

7. Antenna AS-3240/URN & AS-3240A/URN Outline and Installation Drawing. 1979. NAVSEA DWG. No. 5034290, Rev. C, Naval Sea Systems Command, Washington, D.C.

8. Glad, W. E. 1994. NRaD Memorandum Ser 815/9 (8 Apr). Naval Command, Control and Ocean Surveillance Center, RDT&E Division, San Diego, CA.

9. Clements, E. W. 1972. "Shipboard Shock and Navy Devices for its Simulation," NRL Report 7396 (14 Jul), p. 5, Naval Research Laboratory, Washington, D.C.

10. Kiusalaas, J. and R. C. Shaw. 1978. "An Algorithm for Optimal Structural Design with Frequency Constraints," International Journal for Numerical Methods in Engineering, Vol. 13, pp. 283-295.

11. Vanderplaats, G. N. 1984. "ADS - A FORTRAN Program for Automated Design Synthesis," NASA Contractor Report 172460 (Oct).

APPENDIX A: COMPUTER RUN OUTPUT FOR CDF ANTENNA MAST ASSEMBLY WITH TACAN ALONE

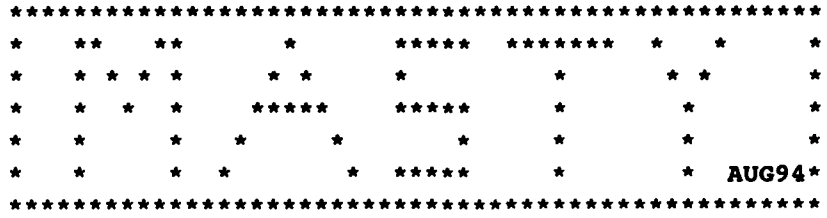

8G/4HZ SHOCK RESPONSE ANALYSIS OF TACAN/CDF ANTENNA ASSEMBLY

I. PHYSICAL PROPERTIES OF TACAN/JTIDS/CDF ANTENNA ASSEMBLY

COMPONENT	WT(#)	INERTIA(#-in2)	C.G.(in)	LENGTH(in)	EI/L3(#/in)
TACAN ANTENNA	115.00	.00	276.00	22.00	-
JTIDS ANTENNA	.00	.00	276.00	28.00	-
TASK LAMP	20.00	.00	259.00	11.00	80.649
EXTENDER TUBE	16.00	.00	237.50	31.00	6.486
CDF MAST	134.00	.00	179.00	84.00	DISTRIBUTION
DIPOLE ARRAY	8.00	.00	214.00	-	-
HEAT SINK 2	10.00	.00	188.75	-	-
HEAT SINK 1	10.00	.00	173.00	-	-
CDF ARRAY	80.00	.00	163.75	-	-
POLE MAST	400.00	.00	69.00	138.00	258.425
UHF ANTENNA 3	40.00	.00	90.00	-	-
UHF ANTENNA 2	40.00	.00	62.00	-	-
UHF ANTENNA 1	40.00	.00	34.00	-	-
TOTAL=	913.00			L= 264.00 (NOT INCLUDING TACAN OR JTIDS)	

WEIGHT AND STIFFNESS DISTRIBUTIONS OF CDF MAST

	PT 1	PT 2	PT 3	PT 4	PT 5	PT 6	PT 7	PT 8	PT 9	PT 10	PT 11
Z-CORD (in)	.000	1.000	1.000	13.750	16.000	19.000	40.500	43.500	57.500	71.000	84.000
O. DIA (in)	17.189	17.189	13.528	13.528	8.753	8.753	7.480	7.202	7.202	5.093	5.093
THICK (in)	2.376	2.376	.795	.795	.614	.614	.599	.468	.477	.734	.734
X-SECT (in2)	110.551	110.551	31.801	31.801	15.700	15.700	12.949	9.901	10.078	10.052	10.052
EI/L3 (#-in)	1724.261	1724.261	358.672	358.672	72.476	72.476	42.806	31.261	31.741	13.610	13.610
SEG LEN (in)		1.000	.000	12.750	2.250	3.000	21.500	3.000	14.000	13.500	13.000
SEG WT (lb)		10.834	.000	39.736	5.141	4.616	30.160	3.356	13.705	13.737	12.806

II. MATERIAL PROPERTIES OF ANTENNA MAST SEGMENTS

SEG NO.	ANTENNA MAST	YOUNGS MOD (psi)	POISSONS RATIO	DENSITY (lb/in3)	YIELD STR (psi)	ULTIM STR (psi)	SECT MOD (in3)
1	POLE MAST	10200000.	.30	.0991	56000.	66000.	88.795
2	CDF MAST	10200000.	.30	.0980	56000.	66000.	95.654 (AT BASE)
3	EXT TUBE	10000000.	.30	.0970	56000.	66000.	5.189
4	TASK LAMP	10000000.	.30	.1760	56000.	66000.	26.929

III. GENERALIZED PROPERTIES BASED ON STATIC DEFLECTION CURVE OF MAST DUE TO ITS OWN WEIGHT

GENERALIZED MASS	GENERALIZED STIFFNESS	GENERALIZED LOAD
.56836E+00	.55251E+03	.80201E+00

DISTRIBUTED	POINTED	ROT INERTIA	FUNDMENTAL FREEQUENCY
.15462E+00	.41374E+00	.00000E+00	.49622E+01 HZ

IV. INITIAL AND FINAL INTEGRATION INFORMATION

T	INT STEPS	DELT	REL ERR
.00000E+00	0	.10000E-03	.00000E+00
.20000E+01	2006	.60000E-03	.42098E-09
.30000E+01	3007	.80000E-03	.26779E-09

13 TIME-HISTORY PLOT VARIABLES HAVE BEEN WRITTEN ON TAPE9

V. MAXIMA/MINIMA OF MOTION HISTORIES AT SPECIFIC LOCATIONS ON MAST

LOCATION	ACCEL (g)		DISP (in)		ANGULAR ACCEL (rad/s2)		ROTATION (deg)	
	MAX	MIN	MAX	MIN	MAX	MIN	MAX	MIN
TACAN ANTENNA	.51466E+02	-.50588E+02	.24917E+02	-.25371E+02	.15590E+03	-.15324E+03	.11192E+02	-.11396E+02
JTIDS ANTENNA	.51466E+02	-.50588E+02	.24917E+02	-.25371E+02	.15590E+03	-.15324E+03	.11192E+02	-.11396E+02
TASK LAMP TIP	.46624E+02	-.45829E+02	.22573E+02	-.22985E+02	.15590E+03	-.15324E+03	.11192E+02	-.11396E+02
EXT TUBE TIP	.42192E+02	-.41473E+02	.20427E+02	-.20800E+02	.15542E+03	-.15277E+03	.11157E+02	-.11361E+02
EXT TUBE BASE	.31096E+02	-.30566E+02	.15055E+02	-.15329E+02	.11434E+03	-.11239E+03	.82085E+01	-.83583E+01
DIPO ANTENNA	.28808E+02	-.28317E+02	.13947E+02	-.14202E+02	.10630E+03	-.10449E+03	.76311E+01	-.77704E+01
HEAT SINK #2	.22652E+02	-.22266E+02	.10967E+02	-.11167E+02	.84589E+02	-.83147E+02	.60725E+01	-.61834E+01
HEAT SINK #1	.19438E+02	-.19106E+02	.94106E+01	-.95824E+01	.73628E+02	-.72372E+02	.52856E+01	-.53821E+01
CDF ANTENNA	.17736E+02	-.17434E+02	.85868E+01	-.87436E+01	.68544E+02	-.67375E+02	.49207E+01	-.50105E+01
CDF MAST BASE	.13488E+02	-.13258E+02	.65300E+01	-.66491E+01	.61422E+02	-.60375E+02	.44094E+01	-.44899E+01
UHF ANTENNA #3	.65422E+01	-.64307E+01	.31673E+01	-.32251E+01	.49068E+02	-.48232E+02	.35225E+01	-.35868E+01
UHF ANTENNA #2	.33588E+01	-.33015E+01	.16261E+01	-.16558E+01	.38055E+02	-.37406E+02	.27319E+01	-.27817E+01
UHF ANTENNA #1	.10970E+01	-.10783E+01	.53110E+00	-.54079E+00	.23460E+02	-.23060E+02	.16841E+01	-.17149E+01
POLE MAST BASE	.79999E+01	-.79999E+01	.00000E+00	.00000E+00	.00000E+00	.00000E+00	.00000E+00	.00000E+00

VI. MAXIMUM/MINIMUM SHEAR FORCES AND BENDING MOMENTS ON MAST

LOCATION	SHEAR (lb)		MOMENT (in-lb)		FLEXURAL STRESS (psi)	
	MAX	MIN	MAX	MIN	MAX	MIN
TACAN ANTENNA	.58177E+04	-.59186E+04	.00000E+00	.00000E+00		
JTIDS ANTENNA	.58177E+04	-.59186E+04	.00000E+00	.00000E+00		
TASK LAMP TIP	.58177E+04	-.59186E+04	.69812E+05	-.71023E+05		
EXT TUBE TIP	.66926E+04	-.68087E+04	.13870E+06	-.14110E+06		
EXT TUBE BASE	.72673E+04	-.73934E+04	.35553E+06	-.36170E+06	.68521E+05	-.69709E+05
DIPO ANTENNA	.74994E+04	-.76295E+04	.41461E+06	-.42180E+06		
HEAT SINK #2	.83595E+04	-.85045E+04	.61235E+06	-.62297E+06		
HEAT SINK #1	.89120E+04	-.90666E+04	.74672E+06	-.75968E+06		
CDF ANTENNA	.10542E+05	-.10725E+05	.83025E+06	-.84465E+06	.27793E+05	-.28275E+05
CDF MAST BASE	.11585E+05	-.11786E+05	.11124E+07	-.11317E+07	.11629E+05	-.11831E+05
UHF ANTENNA #3	.12942E+05	-.13166E+05	.17048E+07	-.17344E+07		
UHF ANTENNA #2	.13334E+05	-.13565E+05	.20733E+07	-.21093E+07		
UHF ANTENNA #1	.13506E+05	-.13740E+05	.24495E+07	-.24920E+07		
POLE MAST BASE	.13543E+05	-.13778E+05	.29096E+07	-.29601E+07	.32768E+05	-.33336E+05

APPENDIX B: COMPUTER RUN OUTPUT FOR CDF ANTENNA MAST ASSEMBLY WITH TACAN AND JTIDS

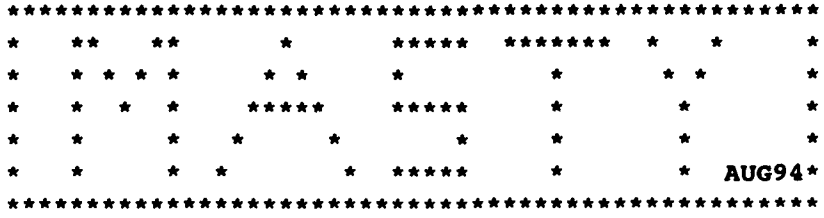

8G/4HZ SHOCK RESPONSE ANALYSIS OF TACAN/JTIDS/CDF ANTENNA ASSEMBLY

I. PHYSICAL PROPERTIES OF TACAN/JTIDS/CDF ANTENNA ASSEMBLY

COMPONENT	WT(#)	INERTIA(#-in2)	C.G.(in)	LENGTH(in)	EI/L3(#/in)
TACAN ANTENNA	115.00	.00	304.00	22.00	-
JTIDS ANTENNA	133.00	.00	276.60	28.00	-
TASK LAMP	20.00	.00	259.00	11.00	80.649
EXTENDER TUBE	16.00	.00	237.50	31.00	6.486
CDF MAST	134.00	.00	179.00	84.00	DISTRIBUTION
DIPOLE ARRAY	8.00	.00	214.00	-	-
HEAT SINK 2	10.00	.00	188.75	-	-
HEAT SINK 1	10.00	.00	173.00	-	-
CDF ARRAY	80.00	.00	163.75	-	-
POLE MAST	400.00	.00	69.00	138.00	258.425
UHF ANTENNA 3	40.00	.00	90.00	-	-
UHF ANTENNA 2	40.00	.00	62.00	-	-
UHF ANTENNA 1	40.00	.00	34.00	-	-

TOTAL= 1046.00 L= 264.00 (NOT INCLUDING TACAN OR JTIDS)

WEIGHT AND STIFFNESS DISTRIBUTIONS OF CDF MAST

	PT 1	PT 2	PT 3	PT 4	PT 5	PT 6	PT 7	PT 8	PT 9	PT 10	PT 11
Z-CORD (in)	.000	1.000	1.000	13.750	16.000	19.000	40.500	43.500	57.500	71.000	84.000
O. DIA (in)	17.189	17.189	13.528	13.528	8.753	8.753	7.480	7.202	7.202	5.093	5.093
THICK (in)	2.376	2.376	.795	.795	.614	.614	.599	.468	.477	.734	.734
X-SECT (in2)	110.551	110.551	31.801	31.801	15.700	15.700	12.949	9.901	10.078	10.052	10.052
EI/L3 (#-in)	1724.261	1724.261	358.672	358.672	72.476	72.476	42.806	31.261	31.741	13.610	13.610
SEG LEN (in)		1.000	.000	12.750	2.250	3.000	21.500	3.000	14.000	13.500	13.000
SEG WT (lb)		10.834	.000	39.736	5.141	4.616	30.160	3.356	13.705	13.737	12.806

II. MATERIAL PROPERTIES OF ANTENNA MAST SEGMENTS

SEG NO.	ANTENNA MAST	YOUNGS MOD (psi)	POISSONS RATIO	DENSITY (lb/in3)	YIELD STR (psi)	ULTIM STR (psi)	SECT MOD (in3)
1	POLE MAST	10200000.	.30	.0991	56000.	66000.	88.795
2	CDF MAST	10200000.	.30	.0980	56000.	66000.	95.654 (AT BASE)
3	EXT TUBE	10000000.	.30	.0970	56000.	66000.	5.189
4	TASK LAMP	10000000.	.30	.1760	56000.	66000.	26.929

III. GENERALIZED PROPERTIES BASED ON STATIC DEFLECTION CURVE OF MAST DUE TO ITS OWN WEIGHT

GENERALIZED MASS	GENERALIZED STIFFNESS	GENERALIZED LOAD
.12126E+01	.50474E+03	.12277E+01

DISTRIBUTED	POINTED	ROT INERTIA	FUNDMENTAL FREEQUENCY
.13049E+00	.10821E+01	.00000E+00	.32471E+01 HZ

IV. INITIAL AND FINAL INTEGRATION INFORMATION

T	INT STEPS	DELT	REL ERR
.00000E+00	0	.10000E-03	.00000E+00
.20000E+01	2005	.10000E-02	.22376E-08
.30000E+01	3005	.10000E-02	.29078E-08

13 PLOT VARIABLES HAS BEEN WRITTEN ON TAPE9

V. MAXIMA/MINIMA OF MOTION HISTORIES AT SPECIFIC MAST LOCATIONS ON MAST

LOCATION	ACCEL (g)		DISP (in)		ANGULAR ACCEL (rad/s2)		ROTATION (deg)	
	MAX	MIN	MAX	MIN	MAX	MIN	MAX	MIN
TACAN ANTENNA	.61092E+02	-.59152E+02	.44504E+02	-.46031E+02	.17522E+03	-.16965E+03	.18927E+02	-.19576E+02
JTIDS ANTENNA	.48667E+02	-.47122E+02	.35453E+02	-.36670E+02	.17522E+03	-.16965E+03	.18927E+02	-.19576E+02
TASK LAMP TIP	.42954E+02	-.41589E+02	.31291E+02	-.32365E+02	.17522E+03	-.16965E+03	.18927E+02	-.19576E+02
EXT TUBE TIP	.37979E+02	-.36772E+02	.27666E+02	-.28616E+02	.17422E+03	-.16868E+03	.18819E+02	-.19464E+02
EXT TUBE BASE	.26154E+02	-.25323E+02	.19053E+02	-.19706E+02	.11300E+03	-.10941E+03	.12206E+02	-.12625E+02
DIPO ANTENNA	.23921E+02	-.23161E+02	.17426E+02	-.18024E+02	.10235E+03	-.99094E+02	.11055E+02	-.11435E+02
HEAT SINK #2	.18230E+02	-.17651E+02	.13280E+02	-.13736E+02	.75347E+02	-.72954E+02	.81390E+01	-.84183E+01
HEAT SINK #1	.15430E+02	-.14940E+02	.11240E+02	-.11626E+02	.62716E+02	-.60724E+02	.67746E+01	-.70070E+01
CDF ANTENNA	.13997E+02	-.13552E+02	.10196E+02	-.10546E+02	.57087E+02	-.55274E+02	.61665E+01	-.63781E+01
CDF MAST BASE	.10531E+02	-.10197E+02	.76719E+01	-.79352E+01	.49594E+02	-.48019E+02	.53571E+01	-.55409E+01
UHF ANTENNA #3	.50080E+01	-.48489E+01	.36482E+01	-.37734E+01	.38365E+02	-.37146E+02	.41441E+01	-.42863E+01
UHF ANTENNA #2	.25411E+01	-.24603E+01	.18511E+01	-.19146E+01	.29195E+02	-.28268E+02	.31536E+01	-.32618E+01
UHF ANTENNA #1	.82032E+00	-.79426E+00	.59758E+00	-.61809E+00	.17670E+02	-.17108E+02	.19086E+01	-.19742E+01
POLE MAST BASE	.80000E+01	-.80000E+01	.00000E+00	.00000E+00	.00000E+00	.00000E+00	.00000E+00	.00000E+00

VI. MAXIMUM/MINIMUM OF SHEAR FORCES AND BENDING MOMENTS AT SPECIFIC LOCATIONS ON MAST

LOCATION	SHEAR (lb)		MOMENT (in-lb)		FLEXURAL STRESS (psi)	
	MAX	MIN	MAX	MIN	MAX	MIN
TACAN ANTENNA	.68024E+04	-.70256E+04	.00000E+00	.00000E+00		
JTIDS ANTENNA	.13070E+05	-.13498E+05	.18639E+06	-.19250E+06		
TASK LAMP TIP	.13070E+05	-.13498E+05	.35106E+06	-.36258E+06		
EXT TUBE TIP	.13855E+05	-.14310E+05	.49924E+06	-.51562E+06		
EXT TUBE BASE	.14348E+05	-.14819E+05	.93687E+06	-.96761E+06	.18056E+06	-.18648E+06
DIPO ANTENNA	.14539E+05	-.15016E+05	.10524E+07	-.10870E+07		
HEAT SINK #2	.15229E+05	-.15729E+05	.14263E+07	-.14731E+07		
HEAT SINK #1	.15663E+05	-.16177E+05	.16683E+07	-.17231E+07		
CDF ANTENNA	.16931E+05	-.17486E+05	.18141E+07	-.18736E+07	.60726E+05	-.62718E+05
CDF MAST BASE	.17736E+05	-.18317E+05	.22583E+07	-.23324E+07	.23609E+05	-.24383E+05
UHF ANTENNA #3	.18771E+05	-.19386E+05	.31374E+07	-.32404E+07		
UHF ANTENNA #2	.19064E+05	-.19690E+05	.36676E+07	-.37879E+07		
UHF ANTENNA #1	.19192E+05	-.19822E+05	.42035E+07	-.43414E+07		
POLE MAST BASE	.19220E+05	-.19850E+05	.48567E+07	-.50160E+07	.54696E+05	-.56490E+05

APPENDIX C: TIME-HISTORY PLOT FILE FOR CDF ANTENNA MAST ASSEMBLY WITH TACAN AND JTIDS

TIME-HISTORY PLOT VARIABLES FOR 8-G/4-HZ SHOCK RESPONSE OF TACAN/JTIDS/CDF ANTENNA MAST ASSEMBLY

TIME (sec)	TAC DISP (in)	TAC ACCEL (g)	EXT SHEAR (lb)	EXT MOMNT (in-lb)	VMS SHEAR (lb)	VMS MOMNT (in-lb)	PMS SHEAR (lb)	PMS MOMNT (in-lb)	PMS ACCEL (g)
.00000E+00	.00000E+00	.00000E+00	.00000E+00	.00000E+00	.00000E+00	.00000E+00	.00000E+00	.00000E+00	.00000E+00
.55000E-02	-.30972E-02	-.15840E+01	.38422E+03	.25088E+05	.47493E+03	.60473E+05	.51467E+03	.13005E+06	.11023E+01
.15500E-01	-.68562E-01	-.43011E+01	.10433E+04	.68123E+05	.12896E+04	.16421E+06	.13975E+04	.35315E+06	.30382E+01
.25500E-01	-.29876E+00	-.65659E+01	.15927E+04	.10399E+06	.19687E+04	.25067E+06	.21334E+04	.53910E+06	.47832E+01
.35500E-01	-.78039E+00	-.81270E+01	.19714E+04	.12872E+06	.24367E+04	.31027E+06	.26406E+04	.66728E+06	.62277E+01
.45500E-01	-.15731E+01	-.87895E+01	.21321E+04	.13921E+06	.26354E+04	.33557E+06	.28559E+04	.72167E+06	.72808E+01
.55500E-01	-.27022E+01	-.84310E+01	.20451E+04	.13353E+06	.25279E+04	.32188E+06	.27394E+04	.69223E+06	.78765E+01
.65500E-01	-.41536E+01	-.70125E+01	.17010E+04	.11107E+06	.21026E+04	.26772E+06	.22785E+04	.57577E+06	.79773E+01
.75500E-01	-.58727E+01	-.45839E+01	.11119E+04	.72603E+05	.13744E+04	.17501E+06	.14894E+04	.37637E+06	.75768E+01
.85500E-01	-.77662E+01	-.12821E+01	.31099E+03	.20306E+05	.38441E+03	.48947E+05	.41657E+03	.10527E+06	.67002E+01
.95500E-01	-.97070E+01	.26771E+01	-.64939E+03	-.42402E+05	-.80269E+03	-.10221E+06	-.86985E+03	-.21981E+06	.54027E+01
.10550E+00	-.11543E+02	.70124E+01	-.17010E+04	-.11107E+06	-.21025E+04	-.26772E+06	-.22785E+04	-.57576E+06	.37656E+01
.11550E+00	-.13108E+02	.11396E+02	-.27644E+04	-.18050E+06	-.34170E+04	-.43509E+06	-.37029E+04	-.93570E+06	.18920E+01
.12550E+00	-.14234E+02	.15478E+02	-.37545E+04	-.24515E+06	-.46408E+04	-.59092E+06	-.50292E+04	-.12708E+07	-.10051E+00
.13550E+00	-.14764E+02	.18909E+02	-.45867E+04	-.29949E+06	-.56695E+04	-.72190E+06	-.61439E+04	-.15525E+07	-.20867E+01
.14550E+00	-.14566E+02	.21367E+02	-.51830E+04	-.33842E+06	-.64065E+04	-.81575E+06	-.69426E+04	-.17544E+07	-.39418E+01
.15550E+00	-.13546E+02	.22583E+02	-.54780E+04	-.35769E+06	-.67713E+04	-.86219E+06	-.73378E+04	-.18542E+07	-.55492E+01
.16550E+00	-.11659E+02	.22363E+02	-.54245E+04	-.35419E+06	-.67051E+04	-.85377E+06	-.72662E+04	-.18361E+07	-.68079E+01
.17550E+00	-.89125E+01	.20601E+02	-.49971E+04	-.32628E+06	-.61768E+04	-.78649E+06	-.66936E+04	-.16914E+07	-.76389E+01
.18550E+00	-.53750E+01	.17295E+02	-.41953E+04	-.27393E+06	-.51857E+04	-.66030E+06	-.56196E+04	-.14201E+07	-.79899E+01
.19550E+00	-.11738E+01	.12552E+02	-.30448E+04	-.19881E+06	-.37635E+04	-.47922E+06	-.40785E+04	-.10306E+07	-.78388E+01
.20550E+00	.35084E+01	.65815E+01	-.15965E+04	-.10424E+06	-.19734E+04	-.25127E+06	-.21385E+04	-.54038E+06	-.71953E+01
.21550E+00	.84420E+01	-.31086E+00	.75405E+02	.49236E+04	.93207E+02	.11868E+05	.10101E+03	.25524E+05	-.60996E+01
.22550E+00	.13362E+02	-.77403E+01	.18776E+04	.12260E+06	.23208E+04	.29551E+06	.25150E+04	.63553E+06	-.46206E+01
.23550E+00	.17982E+02	-.15265E+02	.37029E+04	.24178E+06	.45770E+04	.58280E+06	.49600E+04	.12534E+07	-.28513E+01
.24550E+00	.22014E+02	-.22414E+02	.54370E+04	.35501E+06	.67205E+04	.85573E+06	.72829E+04	.18403E+07	-.90289E+00
.25550E+00	.25182E+02	-.28715E+02	.69653E+04	.45480E+06	.86096E+04	.10963E+07	.93300E+04	.23577E+07	.11023E+01
.26550E+00	.27245E+02	-.33725E+02	.81806E+04	.53415E+06	.10112E+05	.12875E+07	.10958E+05	.27690E+07	.30382E+01
.27550E+00	.28011E+02	-.37062E+02	.89901E+04	.58701E+06	.11112E+05	.14149E+07	.12042E+05	.30430E+07	.47832E+01
.28550E+00	.27350E+02	-.38430E+02	.93221E+04	.60868E+06	.11523E+05	.14672E+07	.12487E+05	.31554E+07	.62277E+01
.29550E+00	.25212E+02	-.37643E+02	.91311E+04	.59622E+06	.11287E+05	.14372E+07	.12231E+05	.30908E+07	.72808E+01
.30550E+00	.21626E+02	-.34638E+02	.84022E+04	.54862E+06	.10386E+05	.13224E+07	.11255E+05	.28440E+07	.78765E+01
.31550E+00	.16709E+02	-.29486E+02	.71525E+04	.46702E+06	.88410E+04	.11257E+07	.95808E+04	.24210E+07	.79773E+01
.32550E+00	.10658E+02	-.22392E+02	.54316E+04	.35466E+06	.67139E+04	.85489E+06	.72757E+04	.18385E+07	.75768E+01

.33550E+00 .37481E+01-.13686E+02 .33198E+04 .21676E+06 .41034E+04 .52250E+06 .44468E+04 .11237E+07 .67003E+01
.34550E+00-.36873E+01-.38076E+01 .92361E+03 .60307E+05 .11417E+04 .14537E+06 .12372E+04 .31263E+06 .54027E+01
.35550E+00-.11268E+02 .67156E+01-.16290E+04-.10637E+06-.20136E+04-.25639E+06-.21820E+04-.55139E+06 .37657E+01
.36550E+00-.18588E+02 .17300E+02-.41964E+04-.27400E+06-.51870E+04-.66047E+06-.56211E+04-.14204E+07 .18920E+01
.37550E+00-.25243E+02 .27337E+02-.66311E+04-.43298E+06-.81965E+04-.10437E+07-.88824E+04-.22445E+07-.10047E+00
.38550E+00-.30844E+02 .36231E+02-.87886E+04-.57385E+06-.10863E+05-.13832E+07-.11772E+05-.29748E+07-.20867E+01
.39550E+00-.35051E+02 .43434E+02-.10536E+05-.68793E+06-.13023E+05-.16582E+07-.14113E+05-.35662E+07-.39418E+01
.40550E+00-.37586E+02 .48480E+02-.11760E+05-.76786E+06-.14536E+05-.18509E+07-.15752E+05-.39805E+07-.55492E+01
.41550E+00-.38257E+02 .51015E+02-.12375E+05-.80800E+06-.15296E+05-.19477E+07-.16576E+05-.41886E+07-.68079E+01
.42550E+00-.36965E+02 .50820E+02-.12327E+05-.80491E+06-.15237E+05-.19402E+07-.16513E+05-.41726E+07-.76389E+01
.43550E+00-.33718E+02 .47828E+02-.11602E+05-.75752E+06-.14340E+05-.18260E+07-.15540E+05-.39270E+07-.79899E+01
.44550E+00-.28632E+02 .42132E+02-.10220E+05-.66730E+06-.12632E+05-.16085E+07-.13689E+05-.34593E+07-.78389E+01
.45550E+00-.21926E+02 .33981E+02-.82427E+04-.53821E+06-.10189E+05-.12973E+07-.11041E+05-.27900E+07-.71953E+01
.46550E+00-.13914E+02 .23772E+02-.57663E+04-.37651E+06-.71276E+04-.90756E+06-.77240E+04-.19518E+07-.60996E+01
.47550E+00-.49879E+01 .12027E+02-.29173E+04-.19049E+06-.36060E+04-.45916E+06-.39078E+04-.98747E+06-.46206E+01
.48550E+00 .43998E+01-.63377E+00 .15373E+03 .10038E+05 .19003E+03 .24196E+05 .20593E+03 .52037E+05-.28514E+01
.49550E+00 .13762E+02-.13525E+02 .32808E+04 .21422E+06 .40553E+04 .51636E+06 .43946E+04 .11105E+07-.90293E+00
.50550E+00 .22604E+02-.25937E+02 .62915E+04 .41080E+06 .77767E+04 .99022E+06 .84275E+04 .21296E+07 .11022E+01
.51550E+00 .30447E+02-.37173E+02 .90171E+04 .58877E+06 .11146E+05 .14192E+07 .12078E+05 .30522E+07 .30382E+01
.52550E+00 .36859E+02-.46594E+02 .11302E+05 .73798E+06 .13970E+05 .17789E+07 .15139E+05 .38256E+07 .47832E+01
.53550E+00 .41479E+02-.53650E+02 .13014E+05 .84974E+06 .16086E+05 .20483E+07 .17432E+05 .44050E+07 .62276E+01
.54550E+00 .44035E+02-.57920E+02 .14050E+05 .91737E+06 .17366E+05 .22113E+07 .18820E+05 .47556E+07 .72808E+01
.55550E+00 .44362E+02-.59131E+02 .14343E+05 .93654E+06 .17729E+05 .22575E+07 .19213E+05 .48550E+07 .78765E+01
.56550E+00 .42415E+02-.57178E+02 .13870E+05 .90562E+06 .17144E+05 .21830E+07 .18579E+05 .46947E+07 .79773E+01
.57550E+00 .38269E+02-.52135E+02 .12646E+05 .82574E+06 .15632E+05 .19904E+07 .16940E+05 .42806E+07 .75768E+01
.58550E+00 .32117E+02-.44246E+02 .10733E+05 .70079E+06 .13266E+05 .16892E+07 .14376E+05 .36329E+07 .67003E+01
.59550E+00 .24263E+02-.33917E+02 .82273E+04 .53720E+06 .10170E+05 .12949E+07 .11020E+05 .27848E+07 .54027E+01
.60550E+00 .15105E+02-.21695E+02 .52625E+04 .34361E+06 .65048E+04 .82826E+06 .70491E+04 .17813E+07 .37657E+01
.61550E+00 .51131E+01-.82326E+01 .19970E+04 .13039E+06 .24684E+04 .31430E+06 .26750E+04 .67595E+06 .18921E+01
.62550E+00-.51956E+01 .57415E+01-.13927E+04-.90937E+05-.17215E+04-.21920E+06-.18655E+04-.47141E+06-.10043E+00
.63550E+00-.15283E+02 .19468E+02-.47225E+04-.30835E+06-.58373E+04-.74327E+06-.63257E+04-.15985E+07-.20866E+01
.64550E+00-.24622E+02 .32200E+02-.78107E+04-.51000E+06-.96545E+04-.12293E+07-.10462E+05-.26438E+07-.39417E+01
.65550E+00-.32722E+02 .43240E+02-.10489E+05-.68486E+06-.12965E+05-.16508E+07-.14050E+05-.35503E+07-.55491E+01
.66550E+00-.39158E+02 .51986E+02-.12610E+05-.82338E+06-.15587E+05-.19847E+07-.16891E+05-.42684E+07-.68079E+01
.67550E+00-.43595E+02 .57962E+02-.14060E+05-.91803E+06-.17379E+05-.22129E+07-.18833E+05-.47590E+07-.76389E+01
.68550E+00-.45802E+02 .60845E+02-.14759E+05-.96370E+06-.18243E+05-.23229E+07-.19770E+05-.49957E+07-.79899E+01
.69550E+00-.45668E+02 .60484E+02-.14671E+05-.95797E+06-.18135E+05-.23091E+07-.19652E+05-.49661E+07-.78389E+01
.70550E+00-.43208E+02 .56907E+02-.13804E+05-.90132E+06-.17063E+05-.21726E+07-.18490E+05-.46724E+07-.71953E+01
.71550E+00-.38559E+02 .50320E+02-.12206E+05-.79700E+06-.15088E+05-.19211E+07-.16350E+05-.41316E+07-.60996E+01

.72550E+00-.31974E+02 .41097E+02-.99689E+04-.65091E+06-.12322E+05-.15690E+07-.13353E+05-.33743E+07-.46207E+01
.73550E+00-.23807E+02 .29752E+02-.72169E+04-.47123E+06-.89206E+04-.11359E+07-.96671E+04-.24428E+07-.28514E+01
.74550E+00-.14496E+02 .16916E+02-.41033E+04-.26792E+06-.50720E+04-.64582E+06-.54964E+04-.13889E+07-.90297E+00
.75550E+00-.45337E+01 .32967E+01-.79968E+03-.52215E+05-.98847E+03-.12586E+06-.10712E+04-.27068E+06 .11022E+01
.76550E+00 .55559E+01-.10360E+02 .25130E+04 .16408E+06 .31062E+04 .39552E+06 .33661E+04 .85061E+06 .30381E+01
.77550E+00 .15247E+02-.23313E+02 .56550E+04 .36924E+06 .69899E+04 .89003E+06 .75748E+04 .19141E+07 .47831E+01
.78550E+00 .24043E+02-.34867E+02 .84578E+04 .55225E+06 .10454E+05 .13312E+07 .11329E+05 .28628E+07 .62276E+01
.79550E+00 .31497E+02-.44414E+02 .10774E+05 .70345E+06 .13317E+05 .16956E+07 .14431E+05 .36467E+07 .72808E+01
.80550E+00 .37244E+02-.51462E+02 .12483E+05 .81509E+06 .15430E+05 .19647E+07 .16721E+05 .42254E+07 .78765E+01
.81550E+00 .41011E+02-.55665E+02 .13503E+05 .88166E+06 .16690E+05 .21252E+07 .18087E+05 .45705E+07 .79773E+01
.82550E+00 .42637E+02-.56840E+02 .13788E+05 .90027E+06 .17043E+05 .21700E+07 .18469E+05 .46669E+07 .75768E+01
.83550E+00 .42076E+02-.54974E+02 .13335E+05 .87071E+06 .16483E+05 .20988E+07 .17862E+05 .45137E+07 .67003E+01
.84550E+00 .39401E+02-.50224E+02 .12183E+05 .79547E+06 .15059E+05 .19174E+07 .16319E+05 .41237E+07 .54028E+01
.85550E+00 .34793E+02-.42903E+02 .10407E+05 .67952E+06 .12864E+05 .16379E+07 .13940E+05 .35226E+07 .37658E+01
.86550E+00 .28534E+02-.33463E+02 .81170E+04 .53000E+06 .10033E+05 .12775E+07 .10873E+05 .27475E+07 .18921E+01
.87550E+00 .20987E+02-.22464E+02 .54491E+04 .35579E+06 .67354E+04 .85763E+06 .72990E+04 .18444E+07-.10039E+00
.88550E+00 .12576E+02-.10542E+02 .25573E+04 .16698E+06 .31610E+04 .40249E+06 .34255E+04 .86559E+06-.20866E+01
.89550E+00 .37574E+01 .16283E+01-.39498E+03-.25790E+05-.48822E+03-.62165E+05-.52907E+03-.13369E+06-.39417E+01
.90550E+00-.49993E+01 .13376E+02-.32446E+04-.21186E+06-.40106E+04-.51067E+06-.43462E+04-.10983E+07-.55491E+01
.91550E+00-.13243E+02 .24069E+02-.58383E+04-.38121E+06-.72166E+04-.91889E+06-.78204E+04-.19762E+07-.68079E+01
.92550E+00-.20561E+02 .33149E+02-.80409E+04-.52503E+06-.99392E+04-.12656E+07-.10771E+05-.27217E+07-.76389E+01
.93550E+00-.26605E+02 .40166E+02-.97429E+04-.63616E+06-.12043E+05-.15334E+07-.13051E+05-.32978E+07-.79899E+01
.94550E+00-.31105E+02 .44796E+02-.10866E+05-.70950E+06-.13431E+05-.17102E+07-.14555E+05-.36780E+07-.78389E+01
.95550E+00-.33883E+02 .46861E+02-.11367E+05-.74221E+06-.14050E+05-.17891E+07-.15226E+05-.38476E+07-.71953E+01
.96550E+00-.34858E+02 .46333E+02-.11239E+05-.73385E+06-.13892E+05-.17689E+07-.15055E+05-.38043E+07-.60996E+01
.97550E+00-.34050E+02 .43334E+02-.10512E+05-.68635E+06-.12993E+05-.16544E+07-.14080E+05-.35580E+07-.46207E+01
.98550E+00-.31576E+02 .38121E+02-.92469E+04-.60378E+06-.11430E+05-.14554E+07-.12386E+05-.31299E+07-.28514E+01
.99550E+00-.27634E+02 .31069E+02-.75364E+04-.49209E+06-.93155E+04-.11861E+07-.10095E+05-.25509E+07-.90301E+00
.10055E+01-.22496E+02 .22669E+02-.54987E+04-.35904E+06-.67968E+04-.86545E+06-.73656E+04-.18612E+07 .10870E+01
.10155E+01-.16485E+02 .13551E+02-.32870E+04-.21462E+06-.40629E+04-.51734E+06-.44029E+04-.11126E+07 .29220E+01
.10255E+01-.99505E+01 .42591E+01-.10331E+04-.67459E+05-.12770E+04-.16261E+06-.13839E+04-.34970E+06 .44862E+01
.10355E+01-.32504E+01-.47006E+01 .11402E+04 .74451E+05 .14094E+04 .17946E+06 .15273E+04 .38595E+06 .56960E+01
.10455E+01 .32706E+01-.12874E+02 .31229E+04 .20391E+06 .38602E+04 .49152E+06 .41832E+04 .10571E+07 .64940E+01
.10555E+01 .92979E+01-.19881E+02 .48226E+04 .31489E+06 .59611E+04 .75903E+06 .64599E+04 .16324E+07 .68510E+01
.10655E+01 .14562E+02-.25430E+02 .61685E+04 .40277E+06 .76247E+04 .97086E+06 .82628E+04 .20880E+07 .67665E+01
.10755E+01 .18848E+02-.29329E+02 .71143E+04 .46452E+06 .87937E+04 .11197E+07 .95296E+04 .24081E+07 .62673E+01
.10855E+01 .22007E+02-.31490E+02 .76384E+04 .49875E+06 .94416E+04 .12022E+07 .10232E+05 .25855E+07 .54047E+01
.10955E+01 .23955E+02-.31925E+02 .77440E+04 .50564E+06 .95721E+04 .12188E+07 .10373E+05 .26212E+07 .42499E+01
.11055E+01 .24674E+02-.30740E+02 .74565E+04 .48687E+06 .92168E+04 .11736E+07 .99880E+04 .25239E+07 .28887E+01

.11155E+01 .24210E+02-.28119E+02 .68207E+04 .44536E+06 .84309E+04 .10735E+07 .91363E+04 .23087E+07 .14154E+01
.11255E+01 .22664E+02-.24309E+02 .58966E+04 .38502E+06 .72887E+04 .92807E+06 .78985E+04 .19959E+07-.73201E-01
.11355E+01 .20181E+02-.19602E+02 .47549E+04 .31047E+06 .58774E+04 .74838E+06 .63693E+04 .16095E+07-.14843E+01
.11455E+01 .16943E+02-.14314E+02 .34721E+04 .22671E+06 .42917E+04 .54647E+06 .46508E+04 .11752E+07-.27344E+01
.11555E+01 .13152E+02-.87621E+01 .21254E+04 .13878E+06 .26272E+04 .33452E+06 .28470E+04 .71942E+06-.37540E+01
.11655E+01 .90225E+01-.32521E+01 .78886E+03 .51509E+05 .97509E+03 .12416E+06 .10567E+04 .26702E+06-.44912E+01
.11755E+01 .47664E+01 .19420E+01-.47107E+03-.30759E+05-.58228E+03-.74142E+05-.63100E+03-.15945E+06-.49144E+01
.11855E+01 .58359E+00 .65894E+01-.15984E+04-.10437E+06-.19757E+04-.25157E+06-.21410E+04-.54103E+06-.50126E+01
.11955E+01-.33469E+01 .10511E+02-.25497E+04-.16648E+06-.31516E+04-.40130E+06-.34154E+04-.86304E+06-.47959E+01
.12055E+01-.68741E+01 .13587E+02-.32957E+04-.21519E+06-.40737E+04-.51871E+06-.44146E+04-.11155E+07-.42929E+01
.12155E+01-.98791E+01 .15752E+02-.38211E+04-.24950E+06-.47231E+04-.60140E+06-.51183E+04-.12934E+07-.35489E+01
.12255E+01-.12278E+02 .17002E+02-.41242E+04-.26929E+06-.50978E+04-.64910E+06-.55243E+04-.13960E+07-.26217E+01
.12355E+01-.14024E+02 .17379E+02-.42155E+04-.27525E+06-.52107E+04-.66348E+06-.56467E+04-.14269E+07-.15777E+01
.12455E+01-.15100E+02 .16968E+02-.41159E+04-.26875E+06-.50875E+04-.64780E+06-.55132E+04-.13932E+07-.48725E+00
.12555E+01-.15523E+02 .15887E+02-.38536E+04-.25162E+06-.47633E+04-.60652E+06-.51619E+04-.13044E+07 .57990E+00
.12655E+01-.15333E+02 .14273E+02-.34622E+04-.22606E+06-.42795E+04-.54491E+06-.46376E+04-.11719E+07 .15588E+01
.12755E+01-.14594E+02 .12275E+02-.29774E+04-.19441E+06-.36803E+04-.46862E+06-.39883E+04-.10078E+07 .23933E+01
.12855E+01-.13380E+02 .10038E+02-.24350E+04-.15899E+06-.30098E+04-.38324E+06-.32617E+04-.82420E+06 .30388E+01
.12955E+01-.11780E+02 .77008E+01-.18680E+04-.12197E+06-.23090E+04-.29400E+06-.25022E+04-.63229E+06 .34645E+01
.13055E+01-.98813E+01 .53816E+01-.13054E+04-.85237E+05-.16136E+04-.20546E+06-.17486E+04-.44186E+06 .36549E+01
.13155E+01-.77747E+01 .31772E+01-.77068E+03-.50322E+05-.95262E+03-.12130E+06-.10323E+04-.26086E+06 .36098E+01
.13255E+01-.55446E+01 .11583E+01-.28097E+03-.18346E+05-.34730E+03-.44223E+05-.37637E+03-.95106E+05 .33435E+01
.13355E+01-.32691E+01-.63035E+00 .15290E+03 .99839E+04 .18900E+03 .24066E+05 .20482E+03 .51756E+05 .28834E+01
.13455E+01-.10171E+01-.21692E+01 .52618E+03 .34357E+05 .65039E+03 .82815E+05 .70482E+03 .17810E+06 .22673E+01
.13555E+01 .11519E+01-.34600E+01 .83929E+03 .54802E+05 .10374E+04 .13210E+06 .11242E+04 .28409E+06 .15411E+01
.13655E+01 .31879E+01-.45215E+01 .10968E+04 .71615E+05 .13557E+04 .17262E+06 .14692E+04 .37125E+06 .75514E+00
.13755E+01 .50499E+01-.53837E+01 .13059E+04 .85271E+05 .16142E+04 .20554E+06 .17493E+04 .44204E+06-.39036E-01
.13855E+01 .67043E+01-.60820E+01 .14753E+04 .96329E+05 .18236E+04 .23220E+06 .19762E+04 .49937E+06-.79186E+00
.13955E+01 .81242E+01-.66512E+01 .16134E+04 .10534E+06 .19942E+04 .25393E+06 .21611E+04 .54610E+06-.14588E+01
.14055E+01 .92874E+01-.71209E+01 .17273E+04 .11279E+06 .21351E+04 .27186E+06 .23138E+04 .58467E+06-.20027E+01
.14155E+01 .10176E+02-.75115E+01 .18221E+04 .11897E+06 .22522E+04 .28677E+06 .24406E+04 .61674E+06-.23960E+01
.14255E+01 .10774E+02-.78309E+01 .18995E+04 .12403E+06 .23480E+04 .29897E+06 .25444E+04 .64296E+06-.26218E+01
.14355E+01 .11070E+02-.80742E+01 .19586E+04 .12788E+06 .24209E+04 .30826E+06 .26235E+04 .66294E+06-.26742E+01
.14455E+01 .11054E+02-.82237E+01 .19948E+04 .13025E+06 .24658E+04 .31397E+06 .26721E+04 .67522E+06-.25585E+01
.14555E+01 .10721E+02-.82513E+01 .20015E+04 .13069E+06 .24740E+04 .31502E+06 .26810E+04 .67748E+06-.22902E+01
.14655E+01 .10070E+02-.81210E+01 .19699E+04 .12863E+06 .24350E+04 .31005E+06 .26387E+04 .66679E+06-.18933E+01
.14755E+01 .91049E+01-.77942E+01 .18906E+04 .12345E+06 .23370E+04 .29757E+06 .25325E+04 .63995E+06-.13986E+01
.14855E+01 .78399E+01-.72334E+01 .17546E+04 .11457E+06 .21688E+04 .27616E+06 .23503E+04 .59391E+06-.84169E+00
.14955E+01 .62962E+01-.64082E+01 .15544E+04 .10150E+06 .19214E+04 .24465E+06 .20822E+04 .52615E+06-.25995E+00

.15055E+01 .45058E+01-.52993E+01 .12854E+04 .83933E+05 .15889E+04 .20232E+06 .17219E+04 .43511E+06 .30936E+00
.15155E+01 .25116E+01-.39031E+01 .94677E+03 .61819E+05 .11703E+04 .14901E+06 .12682E+04 .32047E+06 .83161E+00
.15255E+01 .36744E+00-.22344E+01 .54199E+03 .35389E+05 .66994E+03 .85304E+05 .72599E+03 .18345E+06 .12768E+01
.15355E+01-.18623E+01-.32826E+00 .79625E+02 .51991E+04 .98422E+02 .12532E+05 .10666E+03 .26952E+05 .16211E+01
.15455E+01-.41041E+01 .17597E+01-.42684E+03-.27870E+05-.52761E+03-.67180E+05-.57175E+03-.14448E+06 .18483E+01
.15555E+01-.62776E+01 .39547E+01-.95929E+03-.62637E+05-.11858E+04-.15098E+06-.12850E+04-.32471E+06 .19499E+01
.15655E+01-.82982E+01 .61660E+01-.14957E+04-.97661E+05-.18488E+04-.23541E+06-.20035E+04-.50627E+06 .19258E+01
.15755E+01-.10081E+02 .82909E+01-.20111E+04-.13132E+06-.24859E+04-.31653E+06-.26939E+04-.68074E+06 .17837E+01
.15855E+01-.11544E+02 .10220E+02-.24791E+04-.16187E+06-.30644E+04-.39019E+06-.33208E+04-.83915E+06 .15382E+01
.15955E+01-.12613E+02 .11845E+02-.28733E+04-.18761E+06-.35516E+04-.45222E+06-.38487E+04-.97256E+06 .12096E+01
.16055E+01-.13225E+02 .13063E+02-.31687E+04-.20690E+06-.39167E+04-.49871E+06-.42444E+04-.10725E+07 .82217E+00
.16155E+01-.13335E+02 .13785E+02-.33437E+04-.21833E+06-.41331E+04-.52627E+06-.44789E+04-.11318E+07 .40286E+00
.16255E+01-.12913E+02 .13941E+02-.33816E+04-.22080E+06-.41799E+04-.53223E+06-.45296E+04-.11446E+07-.20817E-01
.16355E+01-.11955E+02 .13487E+02-.32715E+04-.21361E+06-.40438E+04-.51490E+06-.43822E+04-.11074E+07-.42244E+00
.16455E+01-.10478E+02 .12408E+02-.30098E+04-.19652E+06-.37203E+04-.47371E+06-.40316E+04-.10188E+07-.77823E+00
.16555E+01-.85233E+01 .10720E+02-.26004E+04-.16979E+06-.32143E+04-.40927E+06-.34832E+04-.88019E+06-.10684E+01
.16655E+01-.61563E+01 .84724E+01-.20551E+04-.13419E+06-.25403E+04-.32346E+06-.27529E+04-.69564E+06-.12782E+01
.16755E+01-.34633E+01 .57449E+01-.13935E+04-.90991E+05-.17225E+04-.21933E+06-.18666E+04-.47169E+06-.13987E+01
.16855E+01-.54963E+00 .26464E+01-.64194E+03-.41915E+05-.79348E+03-.10103E+06-.85988E+03-.21729E+06-.14266E+01
.16955E+01 .24656E+01-.69052E+00 .16750E+03 .10937E+05 .20704E+03 .26363E+05 .22436E+03 .56696E+05-.13649E+01
.17055E+01 .54538E+01-.41157E+01 .99834E+03 .65186E+05 .12340E+04 .15713E+06 .13373E+04 .33792E+06-.12218E+01
.17155E+01 .82832E+01-.74686E+01 .18116E+04 .11829E+06 .22393E+04 .28514E+06 .24267E+04 .61322E+06-.10100E+01
.17255E+01 .10825E+02-.10586E+02 .25680E+04 .16767E+06 .31742E+04 .40417E+06 .34398E+04 .86921E+06-.74616E+00
.17355E+01 .12959E+02-.13313E+02 .32293E+04 .21086E+06 .39917E+04 .50826E+06 .43257E+04 .10931E+07-.44904E+00
.17455E+01 .14580E+02-.15506E+02 .37613E+04 .24559E+06 .46493E+04 .59199E+06 .50383E+04 .12731E+07-.13869E+00
.17555E+01 .15604E+02-.17047E+02 .41350E+04 .26999E+06 .51112E+04 .65081E+06 .55388E+04 .13996E+07 .16503E+00
.17655E+01 .15972E+02-.17844E+02 .43284E+04 .28262E+06 .53502E+04 .68125E+06 .57979E+04 .14651E+07 .44365E+00
.17755E+01 .15652E+02-.17842E+02 .43280E+04 .28259E+06 .53497E+04 .68118E+06 .57973E+04 .14650E+07 .68115E+00
.17855E+01 .14646E+02-.17023E+02 .41293E+04 .26962E+06 .51041E+04 .64991E+06 .55312E+04 .13977E+07 .86485E+00
.17955E+01 .12985E+02-.15408E+02 .37375E+04 .24404E+06 .46199E+04 .58825E+06 .50065E+04 .12651E+07 .98602E+00
.18055E+01 .10731E+02-.13058E+02 .31675E+04 .20682E+06 .39152E+04 .49853E+06 .42428E+04 .10721E+07 .10402E+01
.18155E+01 .79746E+01-.10070E+02 .24427E+04 .15949E+06 .30193E+04 .38445E+06 .32719E+04 .82680E+06 .10274E+01
.18255E+01 .48305E+01-.65739E+01 .15946E+04 .10412E+06 .19711E+04 .25098E+06 .21360E+04 .53975E+06 .95161E+00
.18355E+01 .14335E+01-.27259E+01 .66122E+03 .43174E+05 .81732E+03 .10407E+06 .88571E+03 .22381E+06 .82064E+00
.18455E+01-.20682E+01 .12988E+01-.31505E+03-.20571E+05-.38942E+03-.49585E+05-.42200E+03-.10664E+06 .64530E+00
.18555E+01-.55198E+01 .53146E+01-.12892E+04-.84175E+05-.15935E+04-.20290E+06-.17268E+04-.43636E+06 .43862E+00
.18655E+01-.87667E+01 .91343E+01-.22157E+04-.14467E+06-.27388E+04-.34873E+06-.29679E+04-.74998E+06 .21493E+00
.18755E+01-.11662E+02 .12579E+02-.30512E+04-.19923E+06-.37715E+04-.48022E+06-.40870E+04-.10328E+07-.11101E-01
.18855E+01-.14073E+02 .15484E+02-.37560E+04-.24525E+06-.46426E+04-.59115E+06-.50311E+04-.12713E+07-.22536E+00

.18955E+01-.15887E+02 .17712E+02-.42965E+04-.28054E+06-.53107E+04-.67622E+06-.57551E+04-.14543E+07-.41517E+00
.19055E+01-.17020E+02 .19156E+02-.46465E+04-.30340E+06-.57435E+04-.73132E+06-.62241E+04-.15728E+07-.56998E+00
.19155E+01-.17416E+02 .19743E+02-.47890E+04-.31270E+06-.59195E+04-.75374E+06-.64148E+04-.16210E+07-.68193E+00
.19255E+01-.17051E+02 .19442E+02-.47162E+04-.30794E+06-.58295E+04-.74227E+06-.63173E+04-.15963E+07-.74618E+00
.19355E+01-.15938E+02 .18265E+02-.44305E+04-.28929E+06-.54765E+04-.69732E+06-.59347E+04-.14997E+07-.76110E+00
.19455E+01-.14122E+02 .16261E+02-.39445E+04-.25755E+06-.48757E+04-.62082E+06-.52836E+04-.13351E+07-.72819E+00
.19555E+01-.11680E+02 .13521E+02-.32797E+04-.21415E+06-.40539E+04-.51619E+06-.43931E+04-.11101E+07-.65182E+00
.19655E+01-.87173E+01 .10167E+02-.24661E+04-.16102E+06-.30483E+04-.38814E+06-.33034E+04-.83474E+06-.53885E+00
.19755E+01-.53635E+01 .63510E+01-.15406E+04-.10059E+06-.19042E+04-.24247E+06-.20636E+04-.52145E+06-.39807E+00
.19855E+01-.17652E+01 .22465E+01-.54492E+03-.35581E+05-.67356E+03-.85765E+05-.72992E+03-.18445E+06-.23956E+00
.19955E+01 .19196E+01-.19614E+01 .47577E+03 .31065E+05 .58808E+03 .74881E+05 .63729E+03 .16104E+06-.73992E-01
.20050E+01 .53527E+01-.58816E+01 .14267E+04 .93156E+05 .17635E+04 .22455E+06 .19111E+04 .48292E+06 .80179E-01
.20150E+01 .87432E+01-.97493E+01 .23649E+04 .15441E+06 .29232E+04 .37221E+06 .31678E+04 .80048E+06 .22970E+00
.20250E+01 .11758E+02-.13182E+02 .31975E+04 .20878E+06 .39523E+04 .50325E+06 .42830E+04 .10823E+07 .35768E+00
.20350E+01 .14266E+02-.16026E+02 .38875E+04 .25383E+06 .48053E+04 .61186E+06 .52073E+04 .13159E+07 .45725E+00
.20450E+01 .16157E+02-.18159E+02 .44048E+04 .28761E+06 .54446E+04 .69327E+06 .59002E+04 .14909E+07 .52364E+00
.20550E+01 .17348E+02-.19487E+02 .47269E+04 .30864E+06 .58428E+04 .74397E+06 .63317E+04 .16000E+07 .55436E+00
.20650E+01 .17790E+02-.19955E+02 .48405E+04 .31606E+06 .59832E+04 .76184E+06 .64838E+04 .16384E+07 .54927E+00
.20750E+01 .17463E+02-.19547E+02 .47415E+04 .30960E+06 .58609E+04 .74627E+06 .63513E+04 .16049E+07 .51043E+00
.20850E+01 .16384E+02-.18286E+02 .44356E+04 .28962E+06 .54827E+04 .69812E+06 .59415E+04 .15014E+07 .44191E+00
.20950E+01 .14601E+02-.16232E+02 .39373E+04 .25708E+06 .48668E+04 .61969E+06 .52740E+04 .13327E+07 .34940E+00
.21050E+01 .12192E+02-.13480E+02 .32697E+04 .21350E+06 .40416E+04 .51462E+06 .43798E+04 .11067E+07 .23980E+00
.21150E+01 .92652E+01-.10155E+02 .24632E+04 .16084E+06 .30447E+04 .38769E+06 .32995E+04 .83376E+06 .12073E+00
.21250E+01 .59470E+01-.64064E+01 .15540E+04 .10147E+06 .19208E+04 .24458E+06 .20816E+04 .52600E+06 .20399E-04
.21350E+01 .23820E+01-.24008E+01 .58235E+03 .38024E+05 .71983E+03 .91656E+05 .78006E+03 .19712E+06-.11477E+00
.21450E+01-.12754E+01 .16862E+01-.40901E+03-.26706E+05-.50557E+03-.64375E+05-.54787E+03-.13844E+06-.21683E+00
.21550E+01-.48680E+01 .56767E+01-.13770E+04-.89911E+05-.17021E+04-.21673E+06-.18445E+04-.46609E+06-.30046E+00
.21650E+01-.82422E+01 .93992E+01-.22800E+04-.14887E+06-.28182E+04-.35884E+06-.30540E+04-.77173E+06-.36140E+00
.21750E+01-.11254E+02 .12695E+02-.30795E+04-.20108E+06-.38065E+04-.48469E+06-.41250E+04-.10424E+07-.39699E+00
.21850E+01-.13778E+02 .15427E+02-.37422E+04-.24435E+06-.46256E+04-.58898E+06-.50127E+04-.12667E+07-.40626E+00
.21950E+01-.15708E+02 .17483E+02-.42407E+04-.27690E+06-.52418E+04-.66745E+06-.56805E+04-.14354E+07-.38993E+00
.22050E+01-.16964E+02 .18779E+02-.45552E+04-.29743E+06-.56306E+04-.71695E+06-.61017E+04-.15419E+07-.35027E+00
.22150E+01-.17498E+02 .19268E+02-.46739E+04-.30518E+06-.57773E+04-.73563E+06-.62607E+04-.15820E+07-.29088E+00
.22250E+01-.17290E+02 .18937E+02-.45935E+04-.29993E+06-.56778E+04-.72296E+06-.61529E+04-.15548E+07-.21640E+00
.22350E+01-.16352E+02 .17806E+02-.43191E+04-.28201E+06-.53387E+04-.67978E+06-.57854E+04-.14619E+07-.13217E+00
.22450E+01-.14729E+02 .15930E+02-.38641E+04-.25231E+06-.47763E+04-.60818E+06-.51760E+04-.13079E+07-.43893E-01
.22550E+01-.12493E+02 .13396E+02-.32495E+04-.21217E+06-.40166E+04-.51143E+06-.43527E+04-.10999E+07 .42773E-01
.22650E+01-.97403E+01 .10316E+02-.25024E+04-.16339E+06-.30931E+04-.39385E+06-.33520E+04-.84702E+06 .12254E+00
.22750E+01-.65907E+01 .68250E+01-.16555E+04-.10810E+06-.20464E+04-.26057E+06-.22176E+04-.56037E+06 .19082E+00

.22850E+01-.31782E+01 .30724E+01-.74528E+03-.48663E+05-.92122E+03-.11730E+06-.99831E+03-.25227E+06 .24394E+00
.22950E+01 .35266E+00-.78216E+00 .18973E+03 .12388E+05 .23452E+03 .29861E+05 .25414E+03 .64220E+05 .27935E+00
.23050E+01 .38535E+01-.45770E+01 .11102E+04 .72493E+05 .13723E+04 .17474E+06 .14872E+04 .37580E+06 .29574E+00
.23150E+01 .71782E+01-.81546E+01 .19781E+04 .12916E+06 .24450E+04 .31133E+06 .26496E+04 .66954E+06 .29303E+00
.23250E+01 .10189E+02-.11368E+02 .27576E+04 .18005E+06 .34085E+04 .43401E+06 .36938E+04 .93339E+06 .27231E+00
.23350E+01 .12762E+02-.14087E+02 .34172E+04 .22312E+06 .42238E+04 .53783E+06 .45773E+04 .11567E+07 .23576E+00
.23450E+01 .14793E+02-.16204E+02 .39306E+04 .25664E+06 .48584E+04 .61863E+06 .52650E+04 .13304E+07 .18640E+00
.23550E+01 .16200E+02-.17635E+02 .42777E+04 .27931E+06 .52876E+04 .67327E+06 .57300E+04 .14479E+07 .12793E+00
.23650E+01 .16927E+02-.18328E+02 .44457E+04 .29028E+06 .54952E+04 .69971E+06 .59551E+04 .15048E+07 .64407E-01
.23750E+01 .16949E+02-.18259E+02 .44290E+04 .28919E+06 .54745E+04 .69708E+06 .59326E+04 .14991E+07 .12163E-04
.23850E+01 .16268E+02-.17437E+02 .42296E+04 .27617E+06 .52281E+04 .66570E+06 .56656E+04 .14317E+07-.61226E-01
.23950E+01 .14916E+02-.15901E+02 .38572E+04 .25186E+06 .47678E+04 .60709E+06 .51667E+04 .13056E+07-.11567E+00
.24050E+01 .12951E+02-.13721E+02 .33282E+04 .21731E+06 .41139E+04 .52383E+06 .44581E+04 .11265E+07-.16029E+00
.24150E+01 .10458E+02-.10988E+02 .26654E+04 .17403E+06 .32946E+04 .41950E+06 .35702E+04 .90218E+06-.19280E+00
.24250E+01 .75414E+01-.78190E+01 .18967E+04 .12384E+06 .23444E+04 .29851E+06 .25406E+04 .64199E+06-.21179E+00
.24350E+01 .43239E+01-.43458E+01 .10542E+04 .68831E+05 .13030E+04 .16591E+06 .14121E+04 .35682E+06-.21673E+00
.24450E+01 .93897E+00-.71195E+00 .17270E+03 .11276E+05 .21347E+03 .27181E+05 .23133E+03 .58456E+05-.20802E+00
.24550E+01-.24734E+01 .29336E+01-.71160E+03-.46464E+05-.87958E+03-.11200E+06-.95318E+03-.24086E+06-.18687E+00
.24650E+01-.57729E+01 .64423E+01-.15627E+04-.10204E+06-.19316E+04-.24595E+06-.20932E+04-.52895E+06-.15518E+00
.24750E+01-.88244E+01 .96723E+01-.23462E+04-.15319E+06-.29001E+04-.36927E+06-.31427E+04-.79415E+06-.11545E+00
.24850E+01-.11503E+02 .12494E+02-.30306E+04-.19788E+06-.37460E+04-.47698E+06-.40594E+04-.10258E+07-.70512E-01
.24950E+01-.13701E+02 .14793E+02-.35884E+04-.23431E+06-.44356E+04-.56479E+06-.48067E+04-.12146E+07-.23417E-01
.25050E+01-.15330E+02 .16481E+02-.39978E+04-.26104E+06-.49416E+04-.62921E+06-.53551E+04-.13532E+07 .22818E-01
.25150E+01-.16323E+02 .17490E+02-.42426E+04-.27702E+06-.52441E+04-.66774E+06-.56830E+04-.14361E+07 .65374E-01
.25250E+01-.16644E+02 .17783E+02-.43135E+04-.28165E+06-.53318E+04-.67891E+06-.57780E+04-.14601E+07 .10180E+00
.25350E+01-.16279E+02 .17349E+02-.42084E+04-.27478E+06-.52018E+04-.66235E+06-.56371E+04-.14245E+07 .13014E+00
.25450E+01-.15246E+02 .16209E+02-.39319E+04-.25673E+06-.48601E+04-.61885E+06-.52668E+04-.13309E+07 .14903E+00
.25550E+01-.13590E+02 .14412E+02-.34959E+04-.22827E+06-.43212E+04-.55022E+06-.46828E+04-.11833E+07 .15778E+00
.25650E+01-.11378E+02 .12031E+02-.29184E+04-.19056E+06-.36074E+04-.45933E+06-.39093E+04-.98785E+06 .15633E+00
.25750E+01-.87024E+01 .91654E+01-.22233E+04-.14517E+06-.27481E+04-.34992E+06-.29780E+04-.75254E+06 .14527E+00
.25850E+01-.56742E+01 .59314E+01-.14388E+04-.93945E+05-.17784E+04-.22645E+06-.19272E+04-.48701E+06 .12577E+00
.25950E+01-.24176E+01 .24612E+01-.59701E+03-.38981E+05-.73794E+03-.93963E+05-.79969E+03-.20208E+06 .99443E-01
.26050E+01 .93377E+00-.11042E+01 .26784E+03 .17488E+05 .33107E+03 .42155E+05 .35877E+03 .90659E+05 .68249E-01
.26150E+01 .42427E+01-.46199E+01 .11206E+04 .73172E+05 .13852E+04 .17638E+06 .15011E+04 .37932E+06 .34361E-01
.26250E+01 .73737E+01-.79432E+01 .19268E+04 .12581E+06 .23816E+04 .30326E+06 .25809E+04 .65219E+06 .71718E-05
.26350E+01 .10199E+02-.10940E+02 .26536E+04 .17327E+06 .32800E+04 .41765E+06 .35545E+04 .89820E+06-.32663E-01
.26450E+01 .12603E+02-.13487E+02 .32716E+04 .21362E+06 .40439E+04 .51492E+06 .43823E+04 .11074E+07-.61710E-01
.26550E+01 .14487E+02-.15483E+02 .37557E+04 .24523E+06 .46423E+04 .59111E+06 .50308E+04 .12713E+07-.85514E-01
.26650E+01 .15775E+02-.16846E+02 .40863E+04 .26681E+06 .50510E+04 .64314E+06 .54736E+04 .13832E+07-.10286E+00

.26750E+01 .16415E+02-.17520E+02 .42499E+04 .27750E+06 .52532E+04 .66889E+06 .56927E+04 .14385E+07-.11299E+00
.26850E+01 .16380E+02-.17479E+02 .42398E+04 .27684E+06 .52407E+04 .66730E+06 .56792E+04 .14351E+07-.11563E+00
.26950E+01 .15672E+02-.16723E+02 .40564E+04 .26486E+06 .50140E+04 .63843E+06 .54335E+04 .13730E+07-.11098E+00
.27050E+01 .14320E+02-.15282E+02 .37070E+04 .24205E+06 .45821E+04 .58344E+06 .49655E+04 .12548E+07-.99692E-01
.27150E+01 .12379E+02-.13216E+02 .32058E+04 .20932E+06 .39626E+04 .50456E+06 .42942E+04 .10851E+07-.82788E-01
.27250E+01 .99296E+01-.10608E+02 .25731E+04 .16801E+06 .31806E+04 .40499E+06 .34467E+04 .87097E+06-.61589E-01
.27350E+01 .70716E+01-.75636E+01 .18347E+04 .11980E+06 .22678E+04 .28876E+06 .24576E+04 .62102E+06-.37618E-01
.27450E+01 .39223E+01-.42073E+01 .10206E+04 .66638E+05 .12615E+04 .16063E+06 .13670E+04 .34545E+06-.12493E-01
.27550E+01 .61107E+00-.67580E+00 .16393E+03 .10704E+05 .20263E+03 .25801E+05 .21958E+03 .55487E+05 .12173E-01
.27650E+01-.27262E+01 .28866E+01-.70019E+03-.45719E+05-.86548E+03-.11020E+06-.93791E+03-.23700E+06 .34876E-01
.27750E+01-.59523E+01 .63339E+01-.15364E+04-.10032E+06-.18991E+04-.24181E+06-.20580E+04-.52005E+06 .54308E-01
.27850E+01-.89345E+01 .95246E+01-.23104E+04-.15086E+06-.28558E+04-.36363E+06-.30948E+04-.78203E+06 .69426E-01
.27950E+01-.11550E+02 .12328E+02-.29903E+04-.19525E+06-.36962E+04-.47064E+06-.40055E+04-.10122E+07 .79506E-01
.28050E+01-.13691E+02 .14627E+02-.35480E+04-.23167E+06-.43856E+04-.55843E+06-.47526E+04-.12010E+07 .84172E-01
.28150E+01-.15268E+02 .16327E+02-.39605E+04-.25860E+06-.48955E+04-.62334E+06-.53051E+04-.13406E+07 .83399E-01
.28250E+01-.16217E+02 .17358E+02-.42105E+04-.27492E+06-.52044E+04-.66269E+06-.56399E+04-.14252E+07 .77503E-01
.28350E+01-.16497E+02 .17675E+02-.42874E+04-.27994E+06-.52995E+04-.67479E+06-.57429E+04-.14512E+07 .67099E-01
.28450E+01-.16097E+02 .17264E+02-.41877E+04-.27343E+06-.51762E+04-.65910E+06-.56094E+04-.14175E+07 .53052E-01
.28550E+01-.15032E+02 .16140E+02-.39152E+04-.25564E+06-.48394E+04-.61621E+06-.52444E+04-.13252E+07 .36411E-01
.28650E+01-.13345E+02 .14350E+02-.34808E+04-.22728E+06-.43025E+04-.54784E+06-.46625E+04-.11782E+07 .18332E-01
.28750E+01-.11106E+02 .11964E+02-.29021E+04-.18949E+06-.35872E+04-.45676E+06-.38873E+04-.98231E+06 .41905E-05
.28850E+01-.84063E+01 .90807E+01-.22027E+04-.14382E+06-.27227E+04-.34668E+06-.29505E+04-.74558E+06-.17425E-01
.28950E+01-.53568E+01 .58180E+01-.14113E+04-.92149E+05-.17444E+04-.22212E+06-.18904E+04-.47769E+06-.32921E-01
.29050E+01-.20834E+01 .23100E+01-.56033E+03-.36587E+05-.69261E+03-.88190E+05-.75056E+03-.18966E+06-.45620E-01
.29150E+01 .12790E+01-.12988E+01 .31505E+03 .20571E+05 .38943E+03 .49586E+05 .42201E+03 .10664E+06-.54873E-01
.29250E+01 .45914E+01-.48592E+01 .11787E+04 .76963E+05 .14570E+04 .18552E+06 .15789E+04 .39897E+06-.60277E-01
.29350E+01 .77166E+01-.82239E+01 .19949E+04 .13025E+06 .24658E+04 .31397E+06 .26721E+04 .67523E+06-.61685E-01
.29450E+01 .10525E+02-.11253E+02 .27296E+04 .17823E+06 .33740E+04 .42961E+06 .36563E+04 .92393E+06-.59206E-01
.29550E+01 .12900E+02-.13820E+02 .33524E+04 .21889E+06 .41438E+04 .52763E+06 .44905E+04 .11347E+07-.53184E-01
.29650E+01 .14743E+02-.15819E+02 .38371E+04 .25054E+06 .47430E+04 .60393E+06 .51398E+04 .12988E+07-.44167E-01
.29750E+01 .15977E+02-.17164E+02 .41635E+04 .27186E+06 .51464E+04 .65529E+06 .55770E+04 .14093E+07-.32857E-01
.29850E+01 .16550E+02-.17800E+02 .43177E+04 .28192E+06 .53370E+04 .67956E+06 .57836E+04 .14615E+07-.20069E-01
.29950E+01 .16438E+02-.17698E+02 .42930E+04 .28031E+06 .53065E+04 .67568E+06 .57505E+04 .14531E+07-.66653E-02

REPORT DOCUMENTATION PAGE

Form Approved
OMB No. 0704-0188

1. AGENCY USE ONLY *(Leave blank)*	2. REPORT DATE	3. REPORT TYPE AND DATES COVERED
	September 1994	Final: April–July 1994

4. TITLE AND SUBTITLE
STRUCTURAL EVALUATION OF TACAN/JTIDS/CDF ANTENNA MAST ASSEMBLY

5. FUNDING NUMBERS
CC54
0205604N
DN213105

6. AUTHOR(S)
R. C. Shaw

7. PERFORMING ORGANIZATION NAME(S) AND ADDRESS(ES)
Naval Command, Control and Ocean Surveillance Center (NCCOSC)
RDT&E Division
San Diego, CA 92152–5001

8. PERFORMING ORGANIZATION REPORT NUMBER
TR 1671

9. SPONSORING/MONITORING AGENCY NAME(S) AND ADDRESS(ES)
Space and Naval Warfare Systems Command
PMA/PMW-159
Washington, DC 20363–5100

10. SPONSORING/MONITORING AGENCY REPORT NUMBER

11. SUPPLEMENTARY NOTES

12a. DISTRIBUTION/AVAILABILITY STATEMENT
Approved for public release; distribution is unlimited.

12b. DISTRIBUTION CODE

13. ABSTRACT *(Maximum 200 words)*

This report details an effort to develop an effective computational method to analyze the dynamic behavior of the shipboard antenna mast assembly when subjected to the shock environment caused by a near-miss underwater explosion.

14. SUBJECT TERMS
shipboard antenna mast assembly
TACAN, JTIDS, and CDF antennas
shock and vibration analysis
Rayleigh's method
Kutta-Merson's fourth-order predictor-corrector technique

15. NUMBER OF PAGES
54

16. PRICE CODE

17. SECURITY CLASSIFICATION OF REPORT	18. SECURITY CLASSIFICATION OF THIS PAGE	19. SECURITY CLASSIFICATION OF ABSTRACT	20. LIMITATION OF ABSTRACT
UNCLASSIFIED	UNCLASSIFIED	UNCLASSIFIED	SAME AS REPORT

21a. NAME OF RESPONSIBLE INDIVIDUAL	21b. TELEPHONE *(include Area Code)*	21c. OFFICE SYMBOL
R. C. Shaw	(619) 553-3230	Code 813

INITIAL DISTRIBUTION

Code 0012	Patent Counsel	(1)
Code 0274	Library	(2)
Code 0275	Archive/Stock	(6)
Code 70	T. F. Ball	(1)
Code 75	J. E. Griffin	(1)
Code 752	C. E. Lantz, Jr.	(3)
Code 753	R. W. Major	(1)
Code 753	J. E. Boyns	(3)
Code 753	R. Cozad	(1)
Code 753	C. E. Dempsey	(1)
Code 753	H. B. Simonds	(1)
Code 80	K. D. Regan	(1)
Code 81	R. E. Miller	(1)
Code 813	A. R. Dean	(1)
Code 813	B. D. Calder	(1)
Code 813	R. N. Dahle	(1)
Code 813	M. A. Jones	(1)
Code 813	M. C. McDonald	(1)
Code 813	R. C. Shaw	(5)
Code 813	D. P. Watry	(1)
Code 815	R. K. Fogg, Jr.	(1)
Code 815	J. M. Adams	(1)
Code 815	W. E. Glad	(1)

Defense Technical Information Center
Alexandria, VA 22304–6145 (4)

NCCOSC Washington Liaison Office
Washington, DC 20363–5100

Center for Naval Analyses
Alexandria, VA 22302–0268

Navy Acquisition, Research and Development
Information Center (NARDIC)
Arlington, VA 22244–5114

GIDEP Operations Center
Corona, CA 91718–8000

Office of Naval Research
Arlington, VA 22217–5000

Naval Air Warfare Center
Aircraft Division
Warminster, PA 18974–5000

Space and Naval Warfare Systems Command
2451 Crystal Drive
Arlington, VA 22245–5200 (2)

NCCOSC, ISE West
San Diego, CA 92186

Computer Sciences Corporation
Arlington, VA 22202

Eldyne, Inc.
Dahlgren, VA 22448

Southwest Research Institute
San Antonio, TX 78284